

Binary neutron stars: Einstein's richest laboratory

Luciano Rezzolla

Institute for Theoretical Physics, Frankfurt



Heidelberg (Frankfurt), June 4th 2020



Plan of the talk

- The richness of merging binary neutron stars
- GW spectroscopy: EOS from frequencies
- Magnetic fields and EM counterparts
- Ejected mass and nucleosynthesis
- GW170817: a game changer
- Signatures of quark-hadron phase transitions

The two-body problem in GR

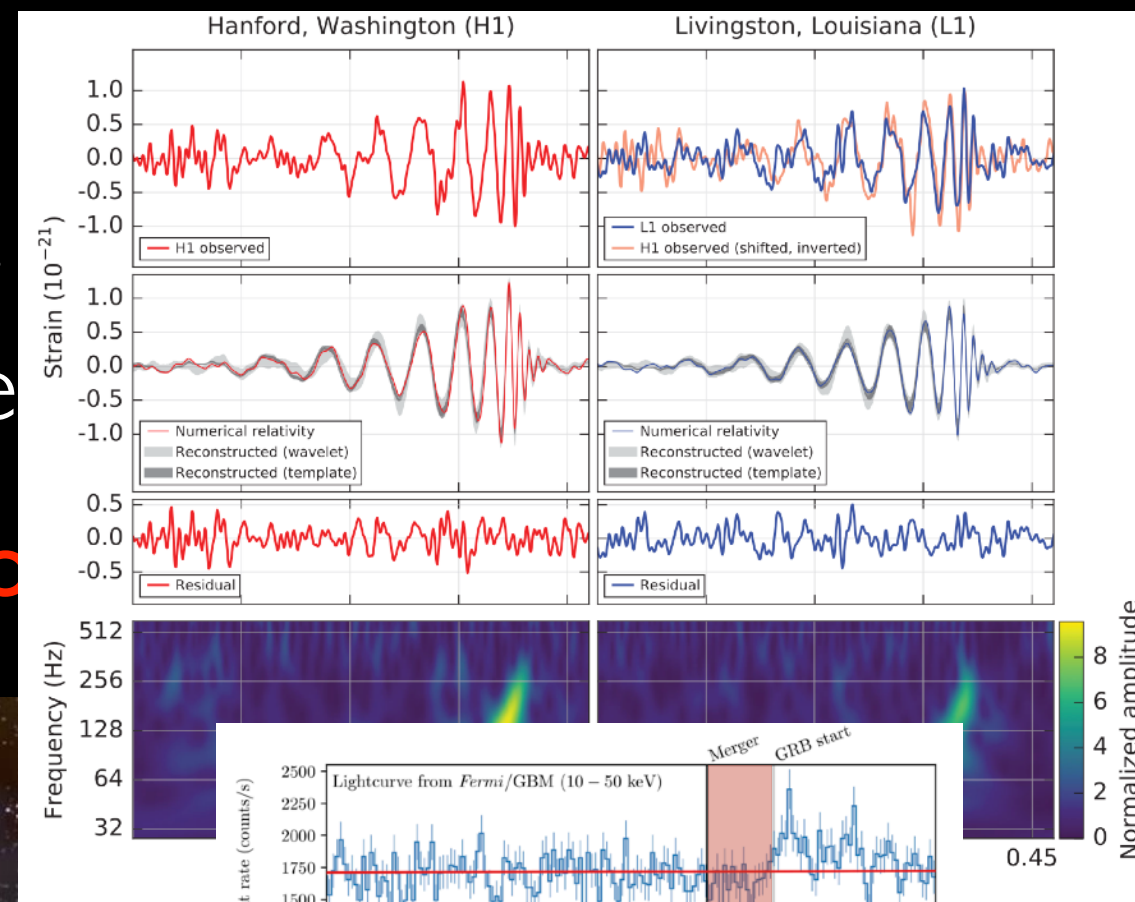
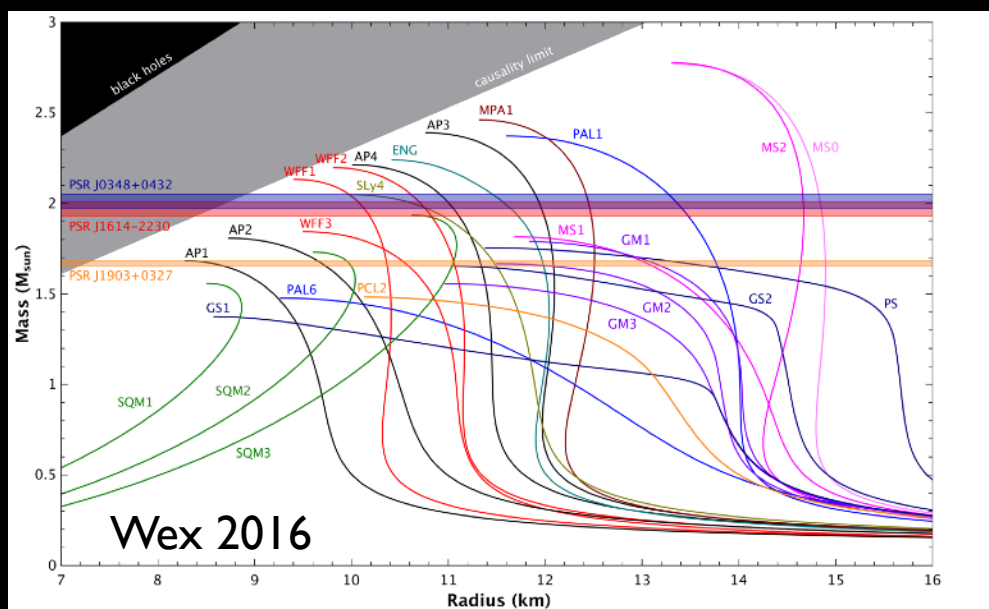
- For black holes the process is very **simple**:

$$\text{BH} + \text{BH} \longrightarrow \text{BH} + \text{GWs}$$

- For NSs the question is more **subtle**: hyper-massive neutron star (HMNS), i.e.

$$\text{NS} + \text{NS} \longrightarrow \text{HMNS} + \dots ? \longrightarrow \text{BH} + \text{torus}$$

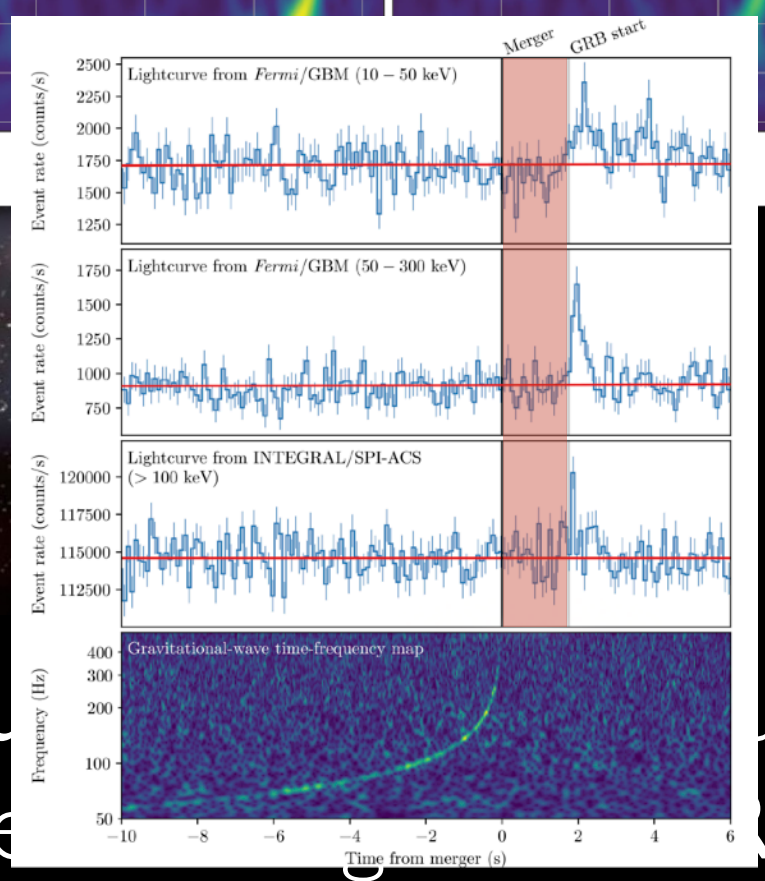
- **HMNS** phase can provide clear information on **EOS**



GW150914

- **BH+torus**
on the ceiling

GW170817



NS
Bs

The two-body problem in GR

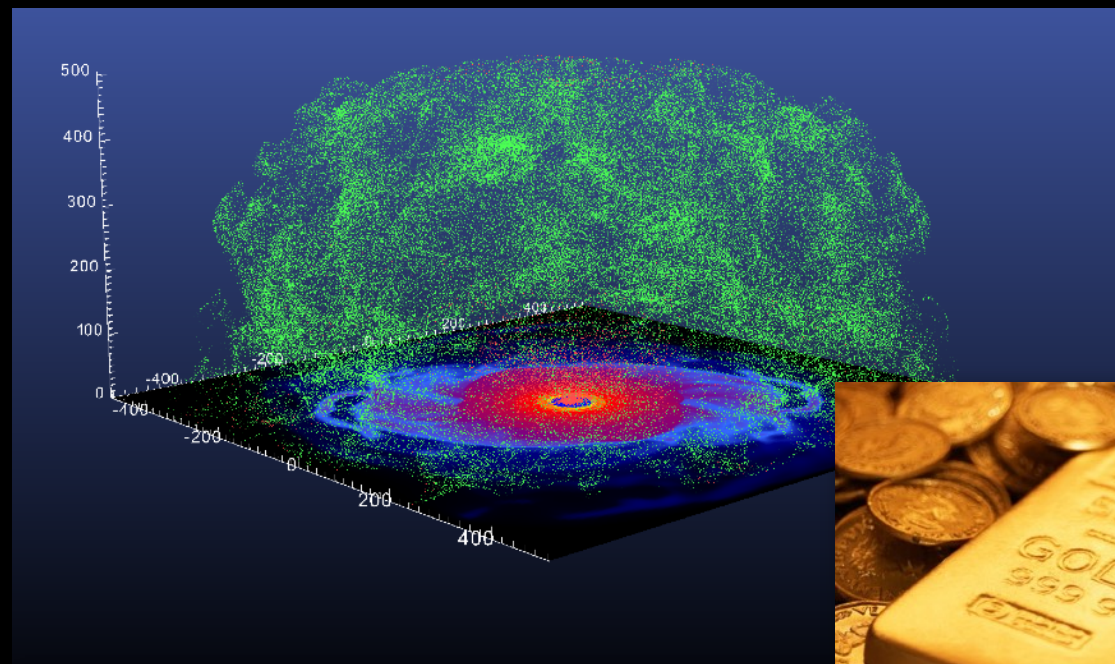
- For black holes the process is very **simple**:



- For NSs the question is more **subtle**: the merger leads to an hyper-massive neutron star (HMNS), ie a metastable equilibrium:



- **ejected matter** undergoes nucleosynthesis of heavy elements



The equations of numerical relativity

$$R_{\mu\nu} - \frac{1}{2}g_{\mu\nu} R = 8\pi T_{\mu\nu}, \text{ (Einstein equations)}$$

$$\nabla_{\mu} T^{\mu\nu} = 0, \text{ (cons. energy/momentum)}$$

$$\nabla_{\mu}(\rho u^{\mu}) = 0, \text{ (cons. rest mass)}$$

$$p = p(\rho, \epsilon, Y_e, \dots), \text{ (equation of state)}$$

$$\nabla_{\nu} F^{\mu\nu} = I^{\mu}, \quad \nabla_{\nu}^* F^{\mu\nu} = 0, \text{ (Maxwell equations)}$$

$$T_{\mu\nu} = T_{\mu\nu}^{\text{fluid}} + T_{\mu\nu}^{\text{EM}} + \dots \text{ (energy - momentum tensor)}$$

The “beauty” disappears quickly when implementing them in numerical codes...

$$\partial_t \tilde{\gamma}_{ij} = -2\alpha \tilde{A}_{ij}^{\text{TF}} + 2\tilde{\gamma}_{k(i}\partial_{j)}\beta^k - \frac{2}{3}\tilde{\gamma}_{ij}\partial_k\beta^k + \beta^k\partial_k\tilde{\gamma}_{ij},$$

$$\begin{aligned} \partial_t \tilde{A}_{ij} = & \phi^2 [-\nabla_i\nabla_j\alpha + \alpha(R_{ij} + \nabla_i Z_j + \nabla_j Z_i - 8\pi S_{ij})]^{\text{TF}} + \alpha\tilde{A}_{ij}(K - 2\Theta) \\ & - 2\alpha\tilde{A}_{il}\tilde{A}_j^l + 2\tilde{A}_{k(i}\partial_{j)}\beta^k - \frac{2}{3}\tilde{A}_{ij}\partial_k\beta^k + \beta^k\partial_k\tilde{A}_{ij}, \end{aligned}$$

$$\partial_t \phi = \frac{1}{3}\alpha\phi K - \frac{1}{3}\phi\partial_k\beta^k + \beta^k\partial_k\phi,$$

$$\partial_t K = -\nabla^i\nabla_i\alpha + \alpha(R + 2\nabla_i Z^i + K^2 - 2\Theta K) + \beta^j\partial_j K - 3\alpha\kappa_1(1 + \kappa_2)\Theta + 4\pi\alpha(S - 3\tau),$$

$$\partial_t \hat{\Gamma}^i = 2\alpha \left(\tilde{\Gamma}_{jk}^i \tilde{A}^{jk} - 3\tilde{A}^{ij} \frac{\partial_j \phi}{\phi} - \frac{2}{3}\tilde{\gamma}^{ij}\partial_j K \right) + 2\tilde{\gamma}^{ki} \left(\alpha\partial_k\Theta - \Theta\partial_k\alpha - \frac{2}{3}\alpha K Z_k \right) - 2\tilde{A}^{ij}\partial_j\alpha$$

$$+ \tilde{\gamma}^{kl}\partial_k\partial_l\beta^i + \frac{1}{3}\tilde{\gamma}^{ik}\partial_k\partial_l\beta^l + \frac{2}{3}\tilde{\Gamma}^i\partial_k\beta^k - \tilde{\Gamma}^k\partial_k\beta^i + 2\kappa_3 \left(\frac{2}{3}\tilde{\gamma}^{ij}Z_j\partial_k\beta^k - \tilde{\gamma}^{jk}Z_j\partial_k\beta^i \right)$$

$$+ \beta^k\partial_k\hat{\Gamma}^i - 2\alpha\kappa_1\tilde{\gamma}^{ij}Z_j - 16\pi\alpha\tilde{\gamma}^{ij}S_j,$$

$$\partial_t \Theta = \frac{1}{2}\alpha \left(R + 2\nabla_i Z^i - \tilde{A}_{ij}\tilde{A}^{ij} + \frac{2}{3}K^2 - 2\Theta K \right) - Z^i\partial_i\alpha + \beta^k\partial_k\Theta - \alpha\kappa_1(2 + \kappa_2)\Theta - 8\pi\alpha\tau,$$

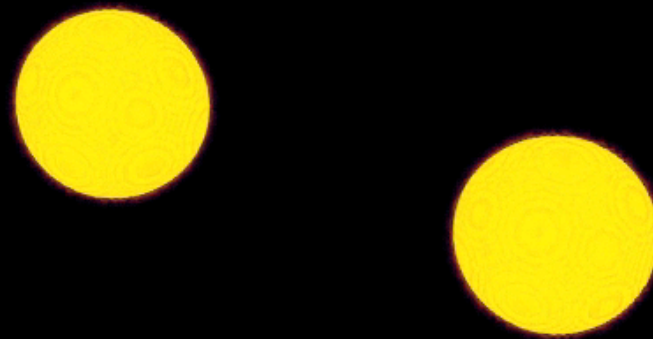
$$\partial_t \alpha = -2\alpha(K - 2\Theta) + \beta^k\partial_k\alpha,$$

$$\partial_t \beta^i = fB^i + \beta^k\partial_k\beta^i,$$

$$\partial_t B^i = \partial_t \hat{\Gamma}^i - \beta^k\partial_k\hat{\Gamma}^i + \beta^k\partial_k B^i - \eta B^i,$$

Total system in 1st-order form has 58 variables

A prototypical simulation with possibly the best code looks like this...



merger \longrightarrow HMNS \longrightarrow $M \approx 2 \times 1.35 M_{\odot}$ BH + torus
LS220 EOS

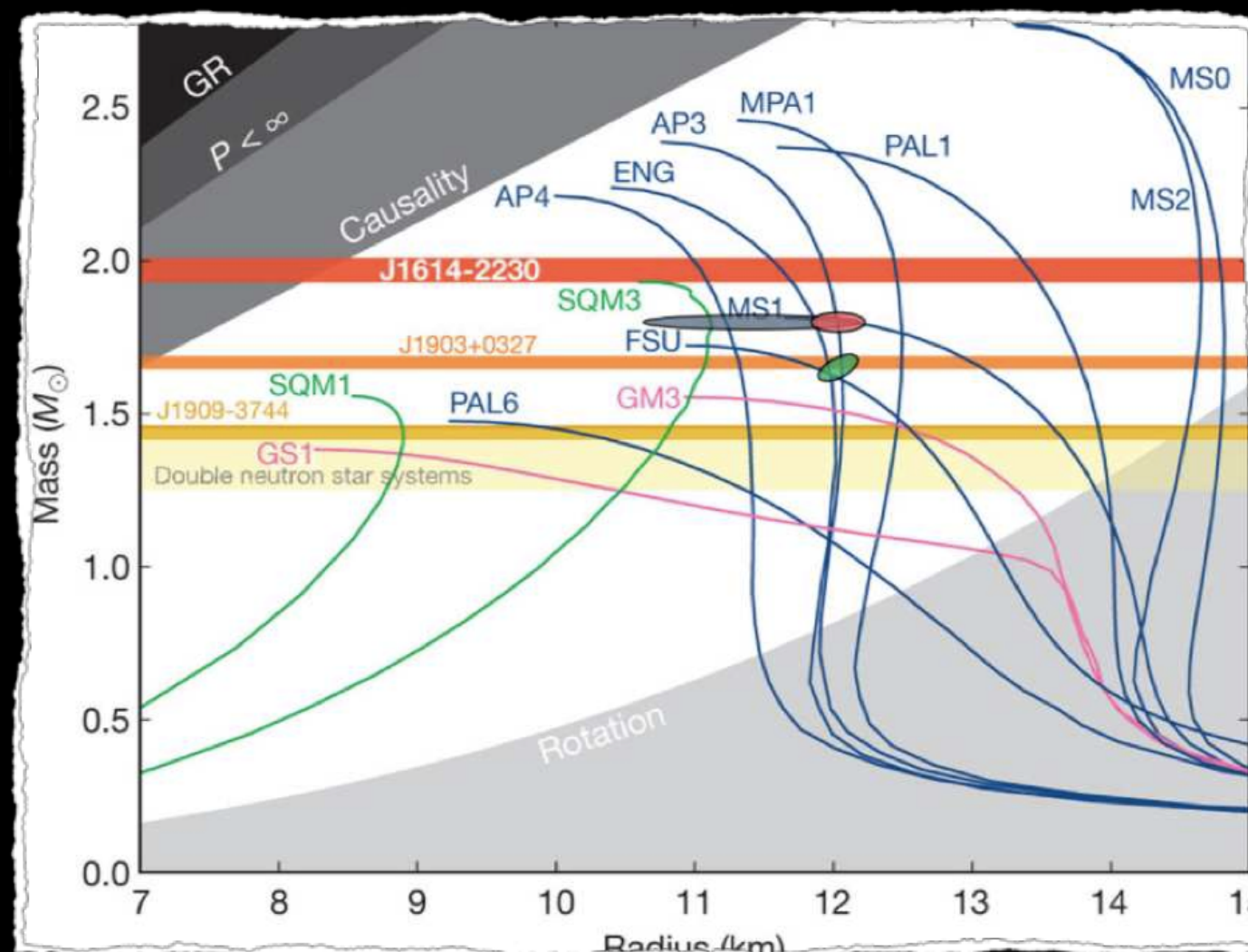
merger \longrightarrow HMNS \longrightarrow BH + torus

Quantitative differences are produced by:

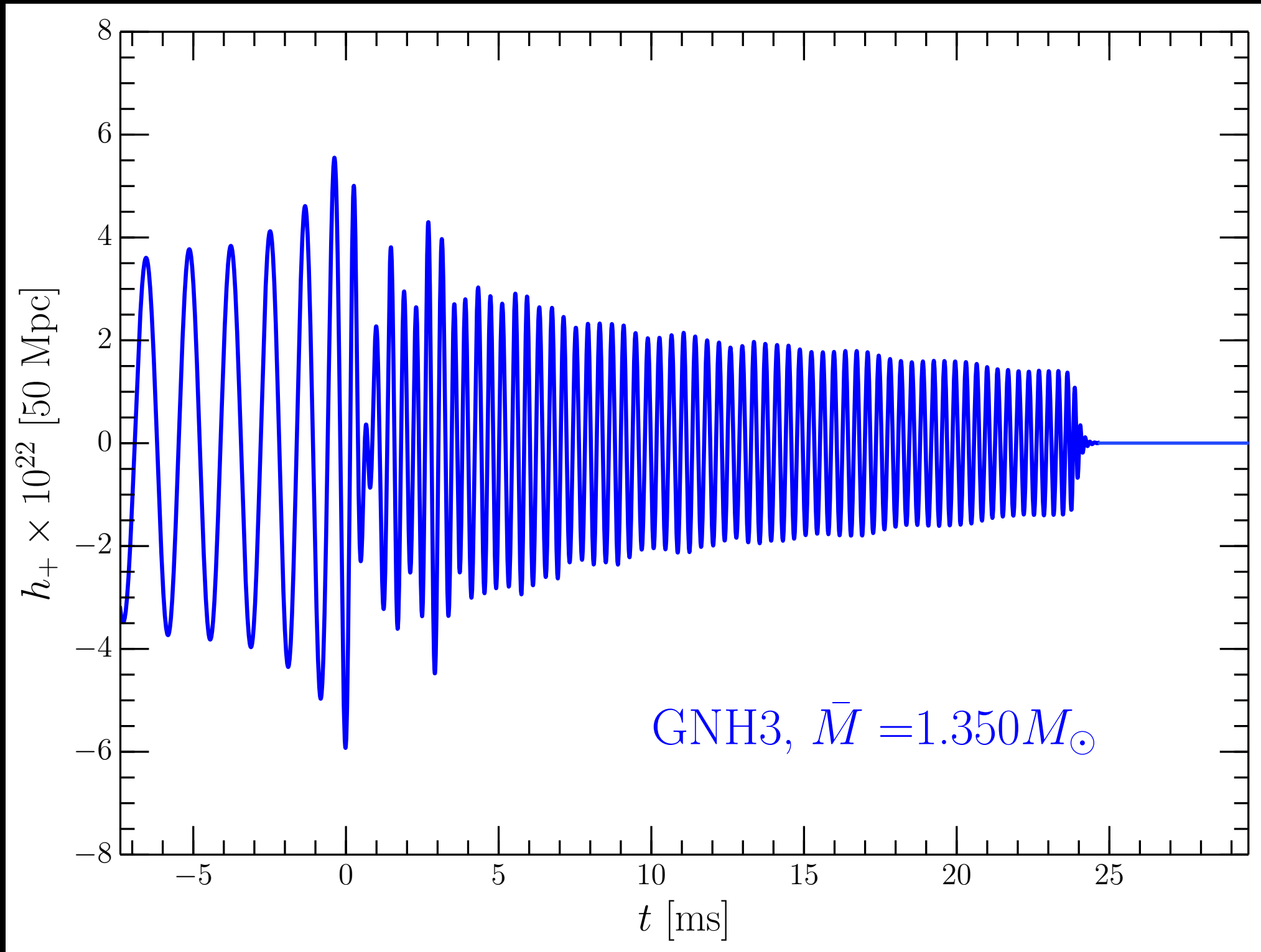
- total **mass** (prompt vs delayed collapse)
- mass **asymmetries** (HMNS and torus)
- soft/stiff **EOS** (inspiral and post-merger)
- **magnetic fields** (equil. and EM emission)
- **radiative** losses (equil. and nucleosynthesis)

GW spectroscopy and how to constrain the EOS

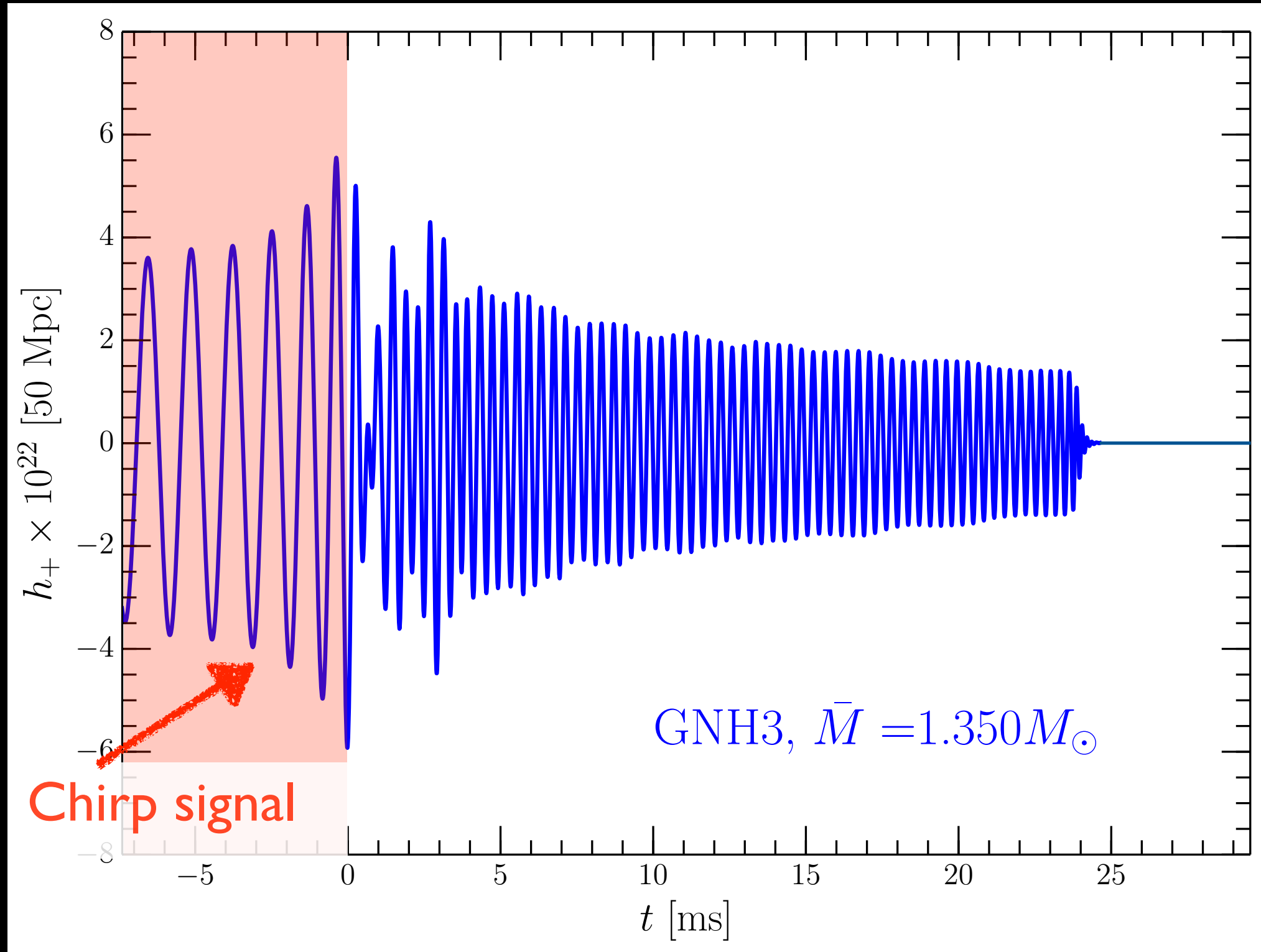
Baiotti, Bose, LR, Takami PRL, PRD (2015-2018)



Anatomy of the GW signal

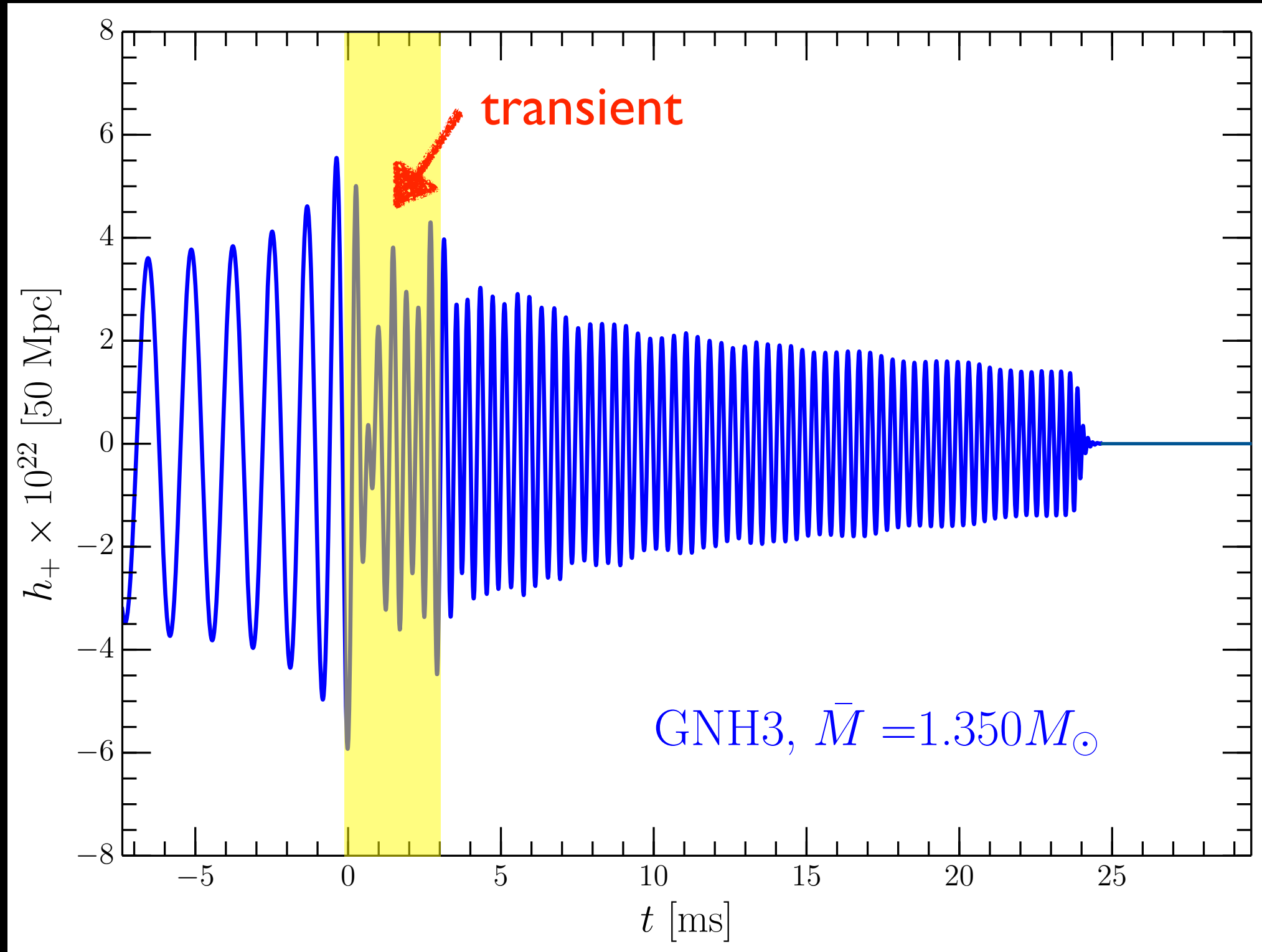


Anatomy of the GW signal



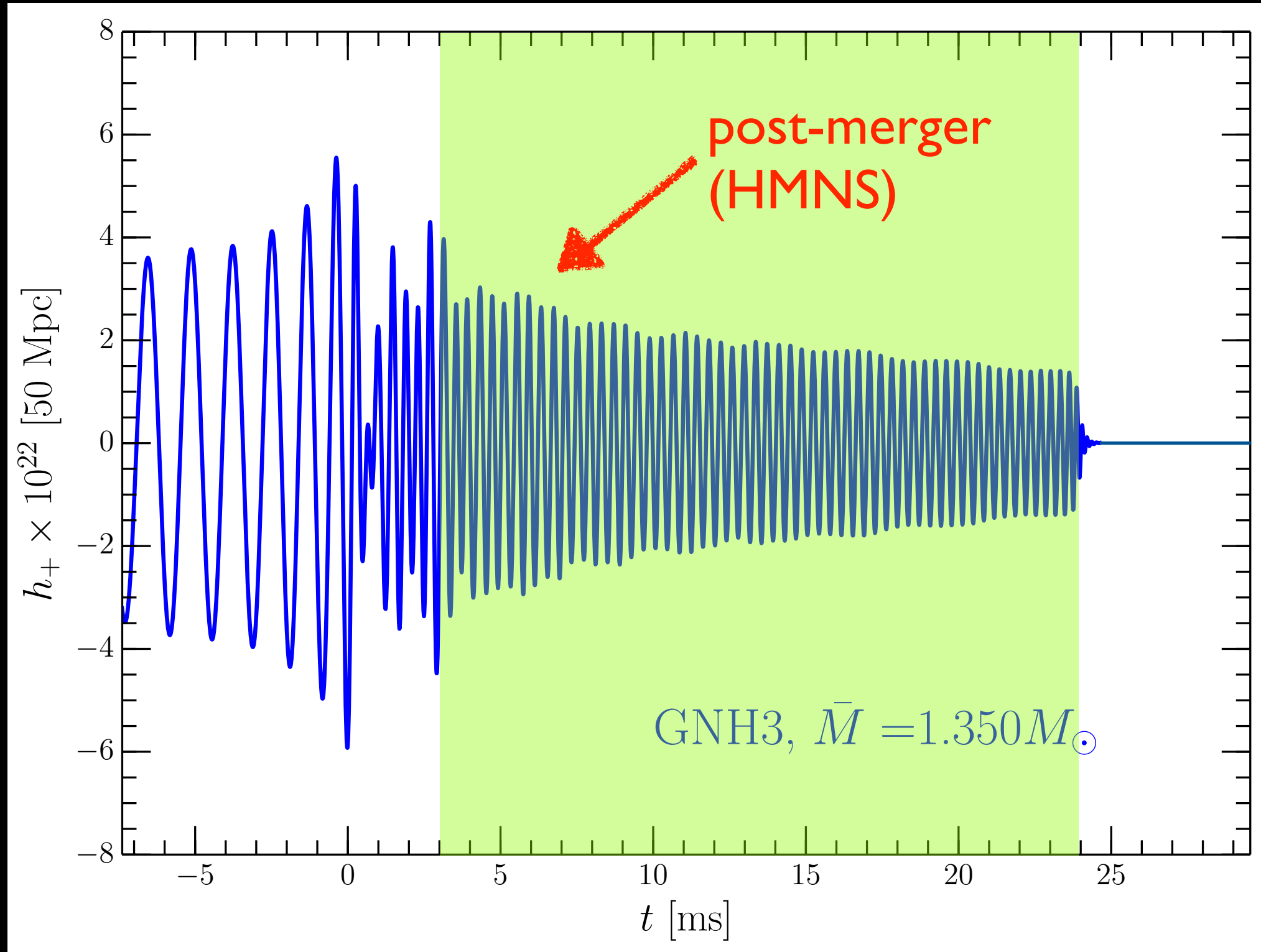
Inspiral: well approximated by PN/EOB; tidal effects important

Anatomy of the GW signal



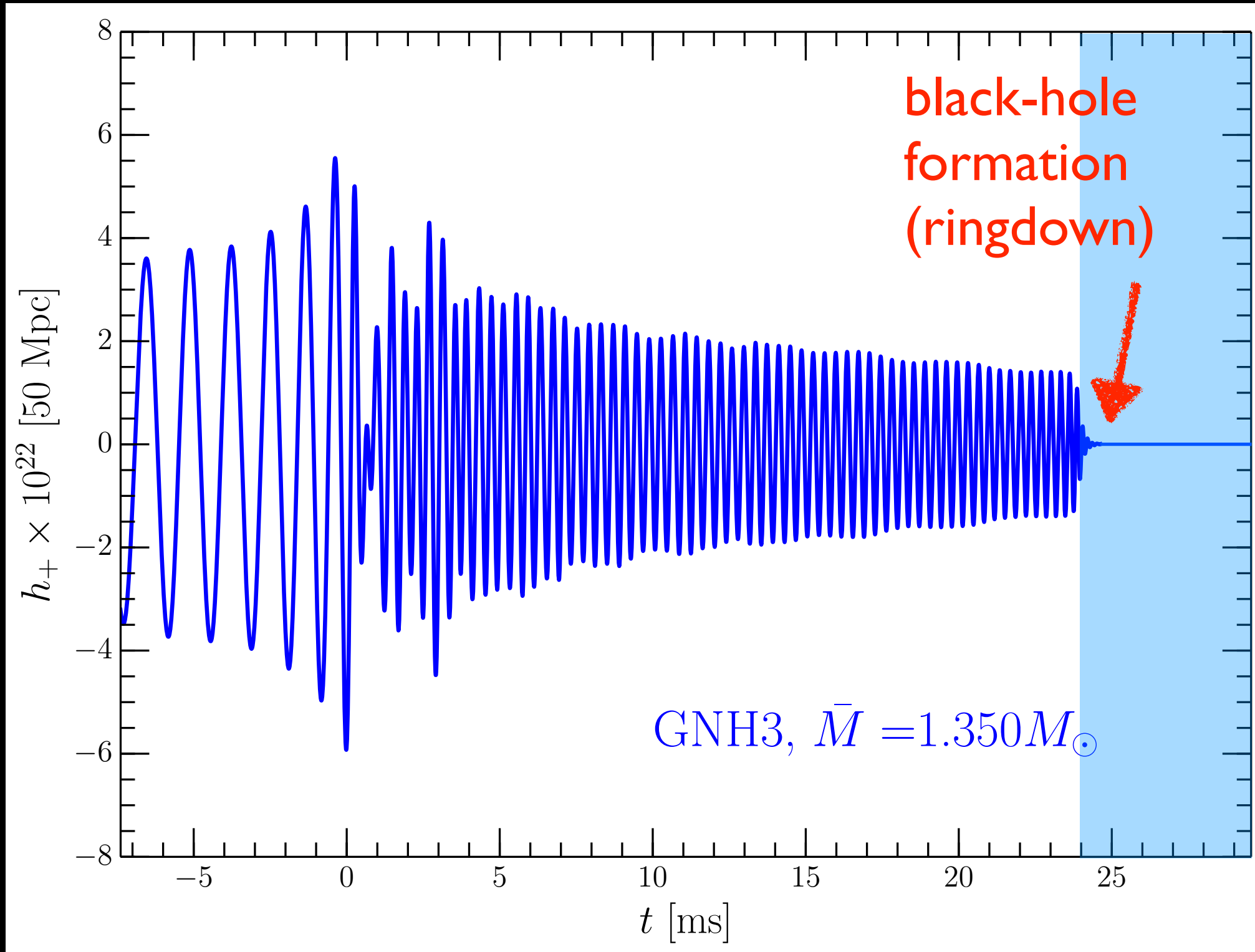
Merger: highly nonlinear but analytic description possible

Anatomy of the GW signal



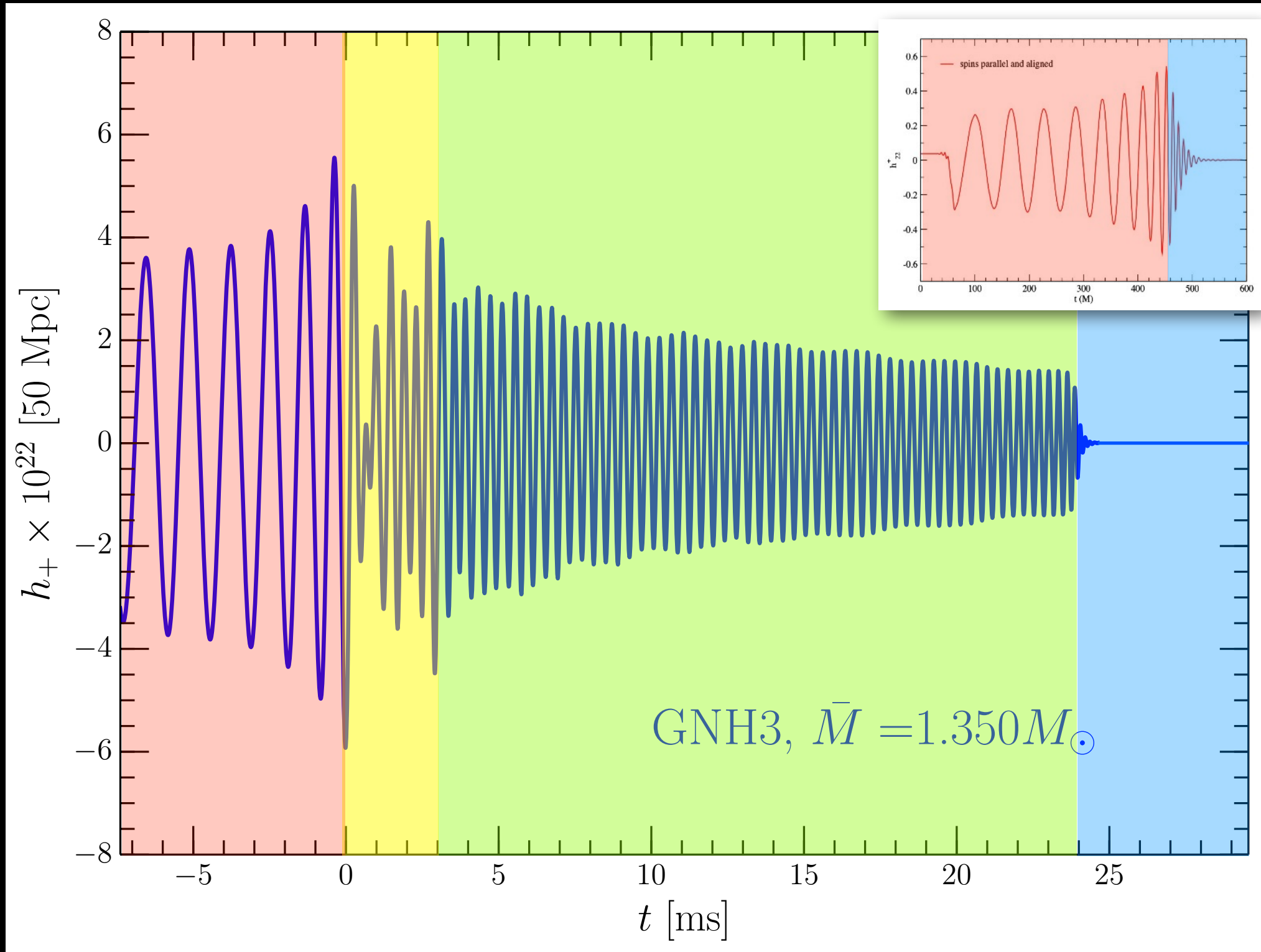
post-merger: quasi-periodic emission of bar-deformed HMNS

Anatomy of the GW signal



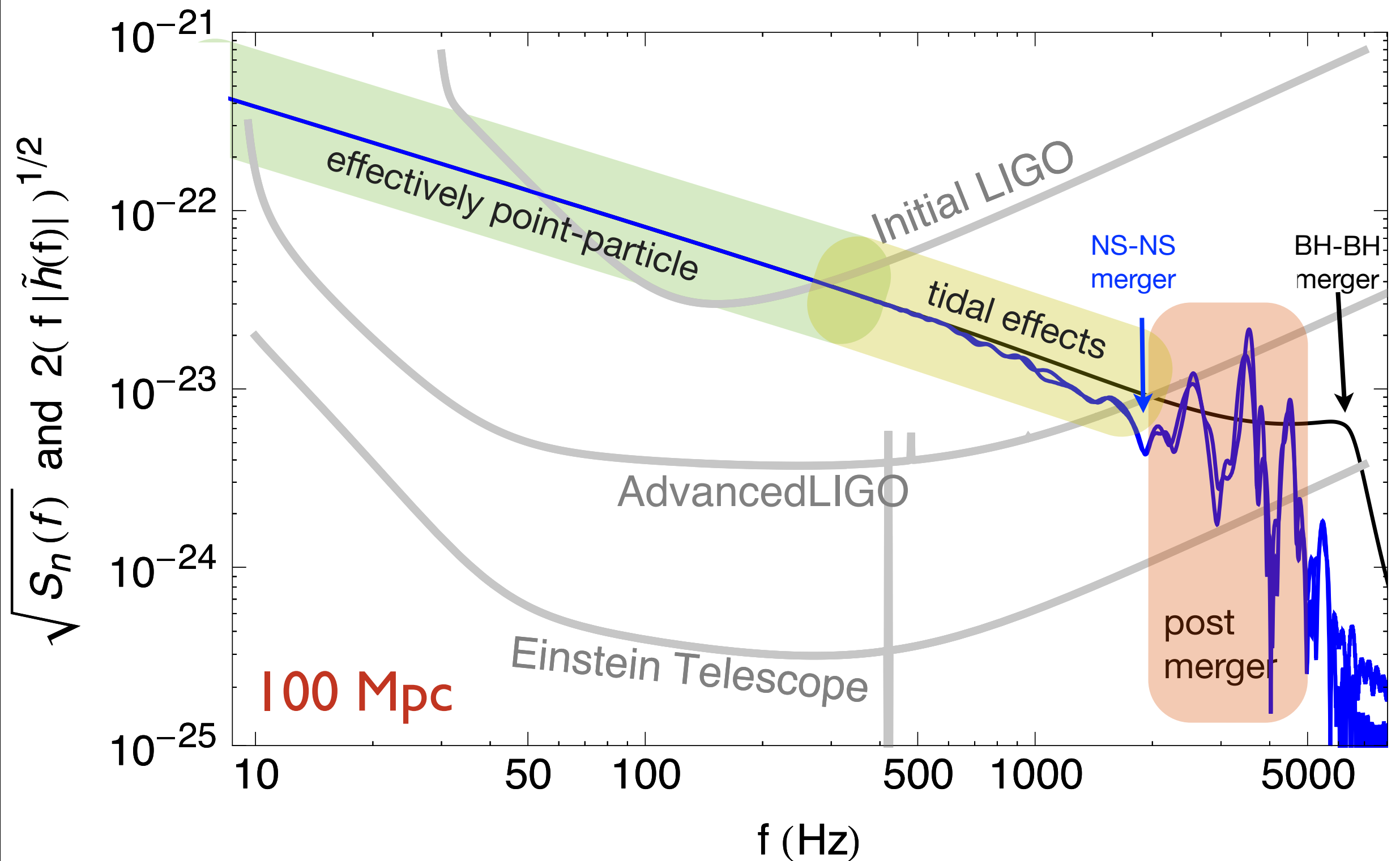
Collapse-ringdown: signal essentially shuts off

Anatomy of the GW signal



Postmerger signal: peculiar of binary NSs

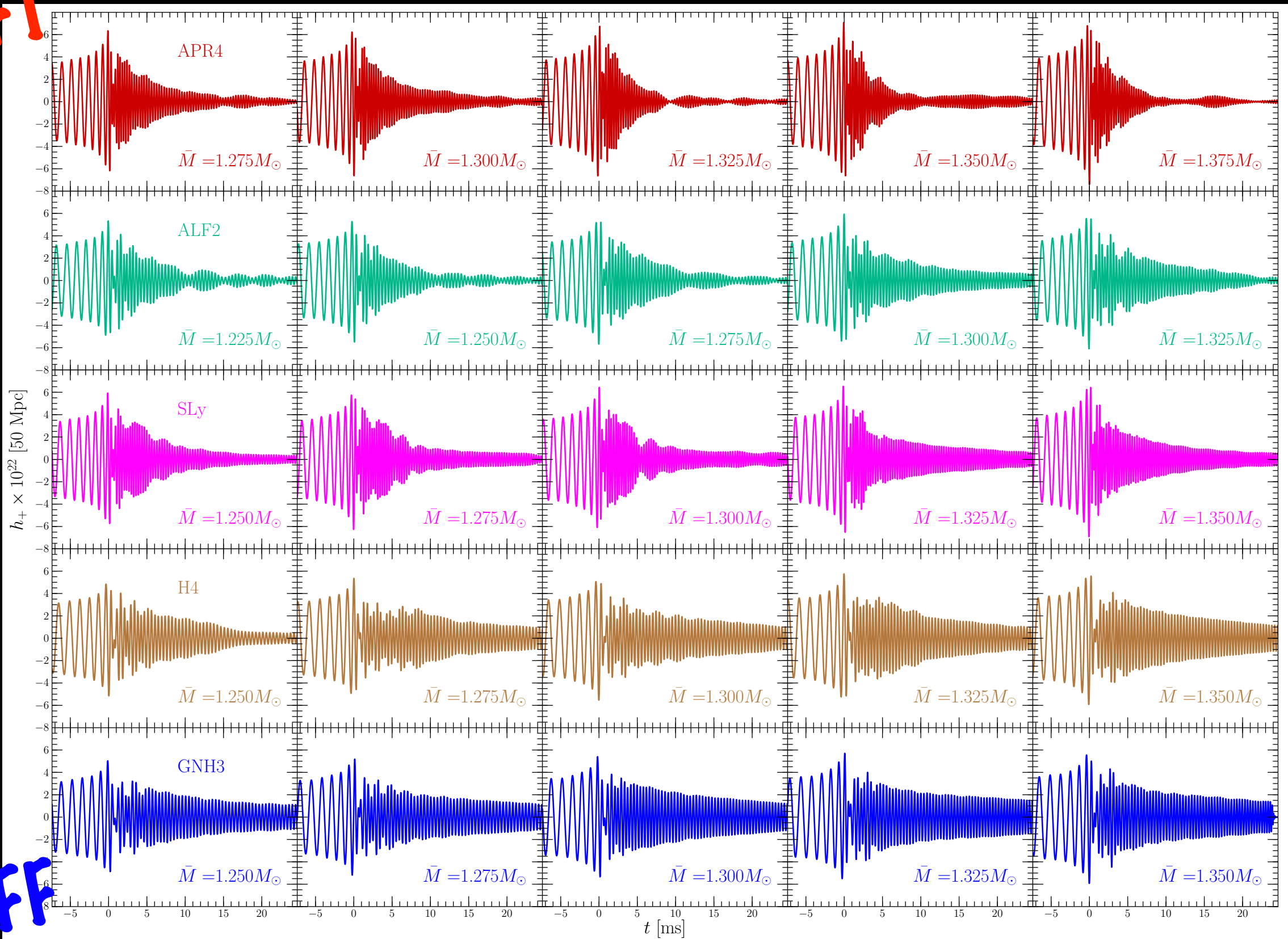
In frequency space



What we can do nowadays

Takami, LR, Baiotti (2014, 2015), LR+ (2016)

SOFT

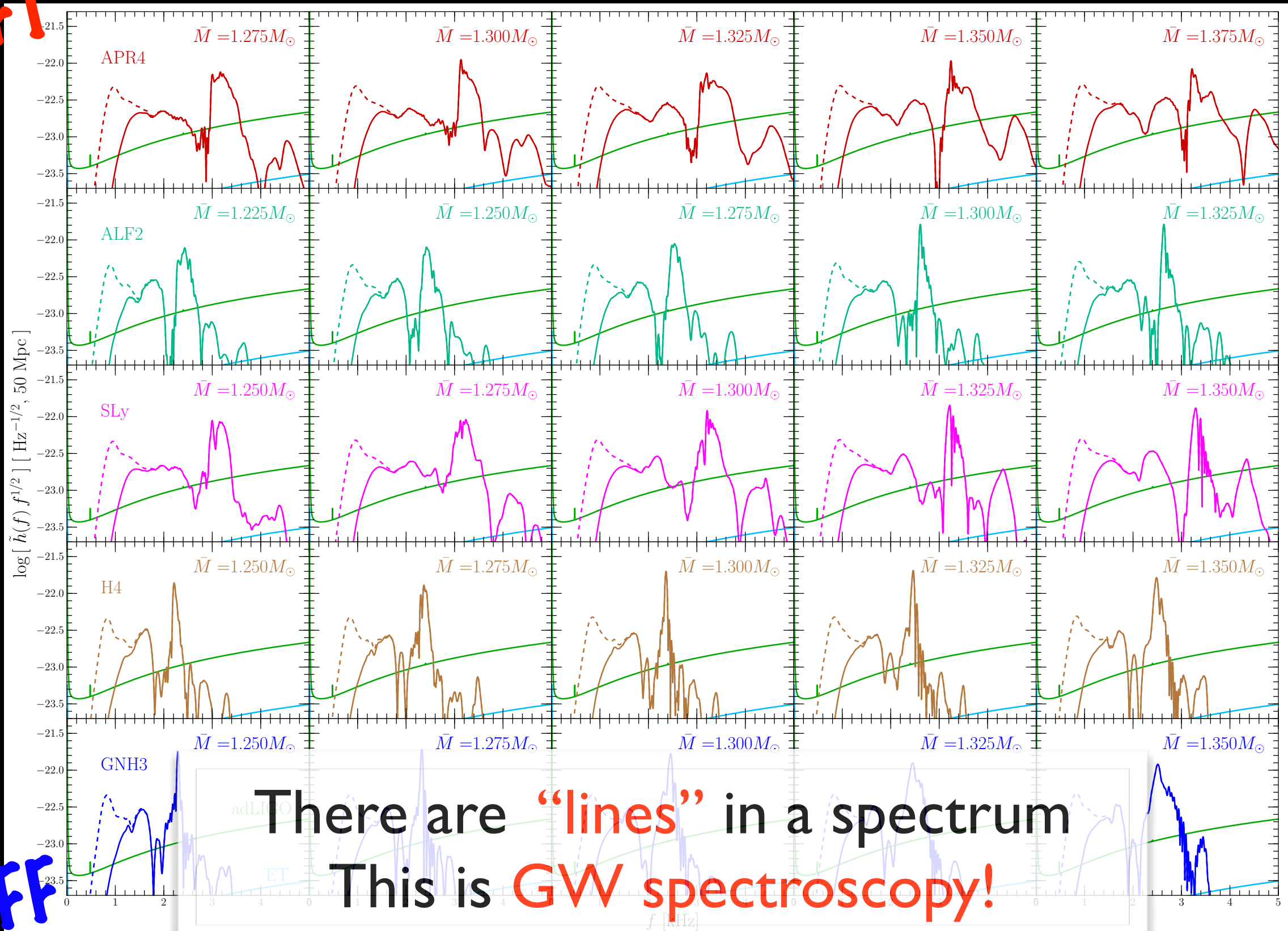


STIFF

Extracting information from the EOS

Takami, LR, Baiotti (2014, 2015), LR+ (2016)

SOFT

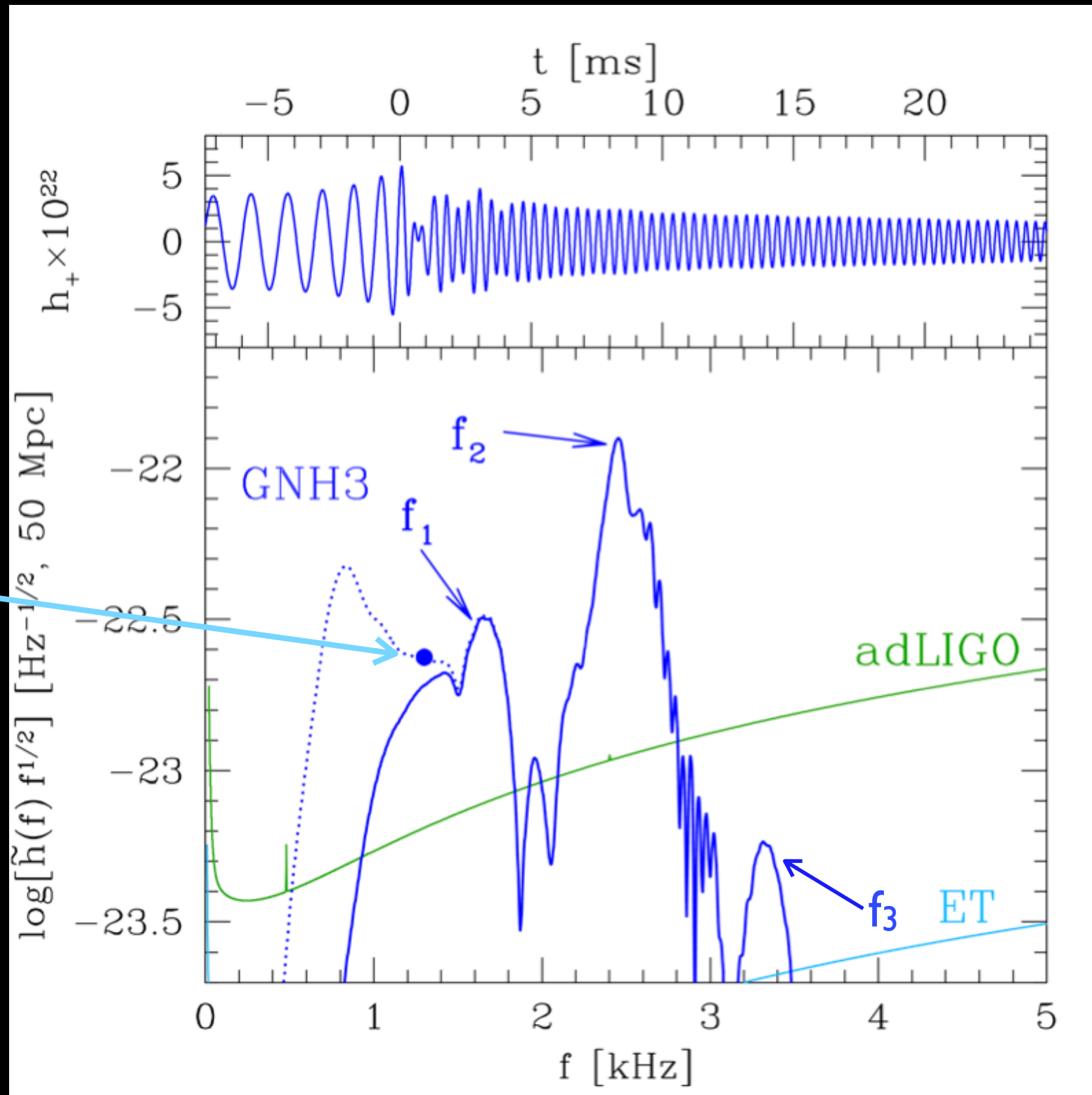


STIFF

A spectroscopic approach to the EOS

Oechslin+2007, Baiotti+2008, Bauswein+ 2011, 2012, Stergioulas+ 2011, Hotokezaka+ 2013, Takami 2014, 2015, Bernuzzi 2014, 2015, Bauswein+ 2015, Clark+ 2016, LR+2016, de Pietri+ 2016, Feo+ 2017, Bose+ 2017 .

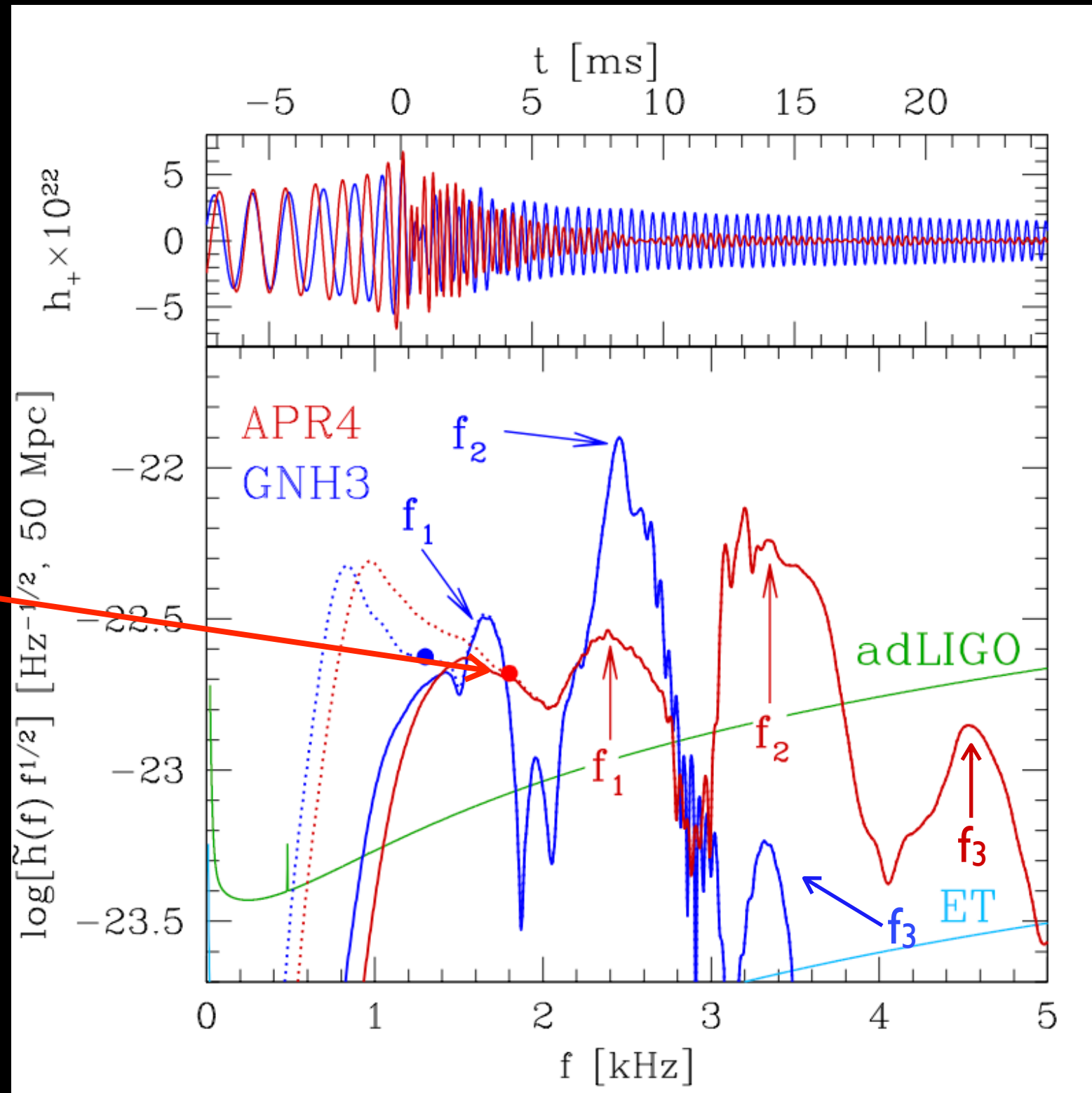
merger
frequency



A spectroscopic approach to the EOS

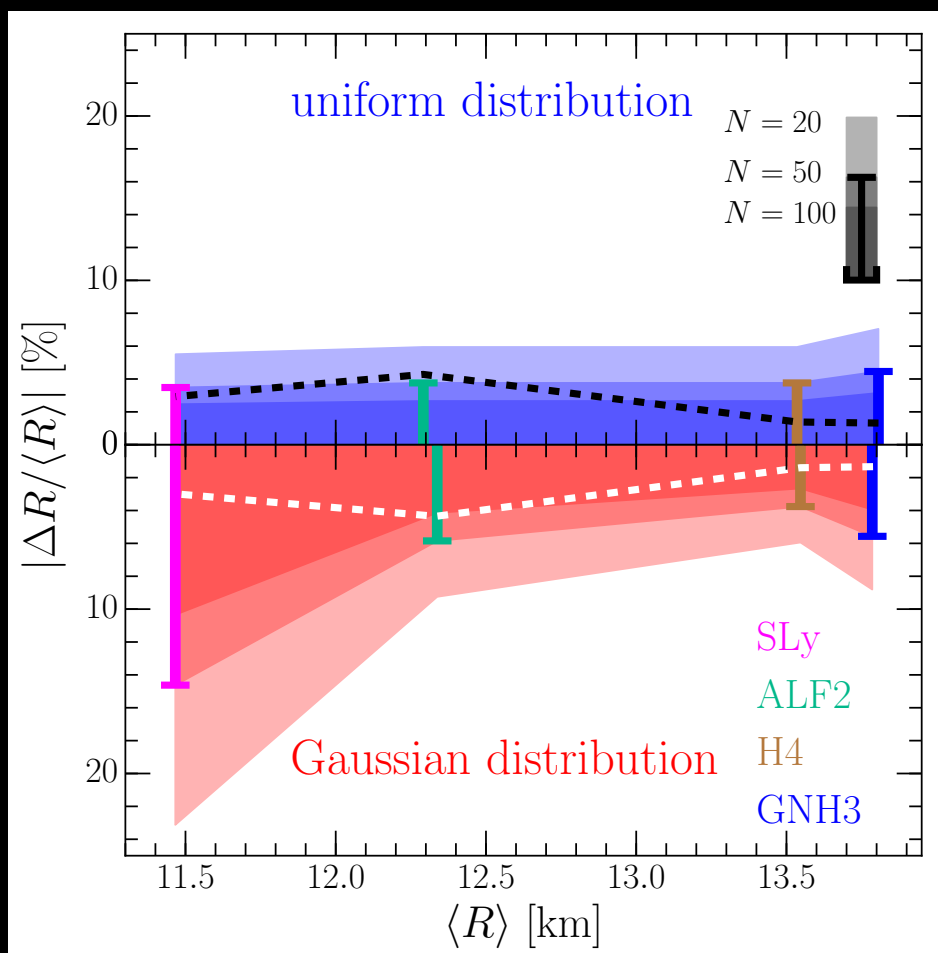
Oechslin+2007, Baiotti+2008, Bauswein+ 2011, 2012, Stergioulas+ 2011, Hotokezaka+ 2013, Takami 2014, 2015, Bernuzzi 2014, 2015, Bauswein+ 2015, Clark+ 2016, LR+2016, de Pietri+ 2016, Feo+ 2017, Bose+ 2017 .

merger
frequency



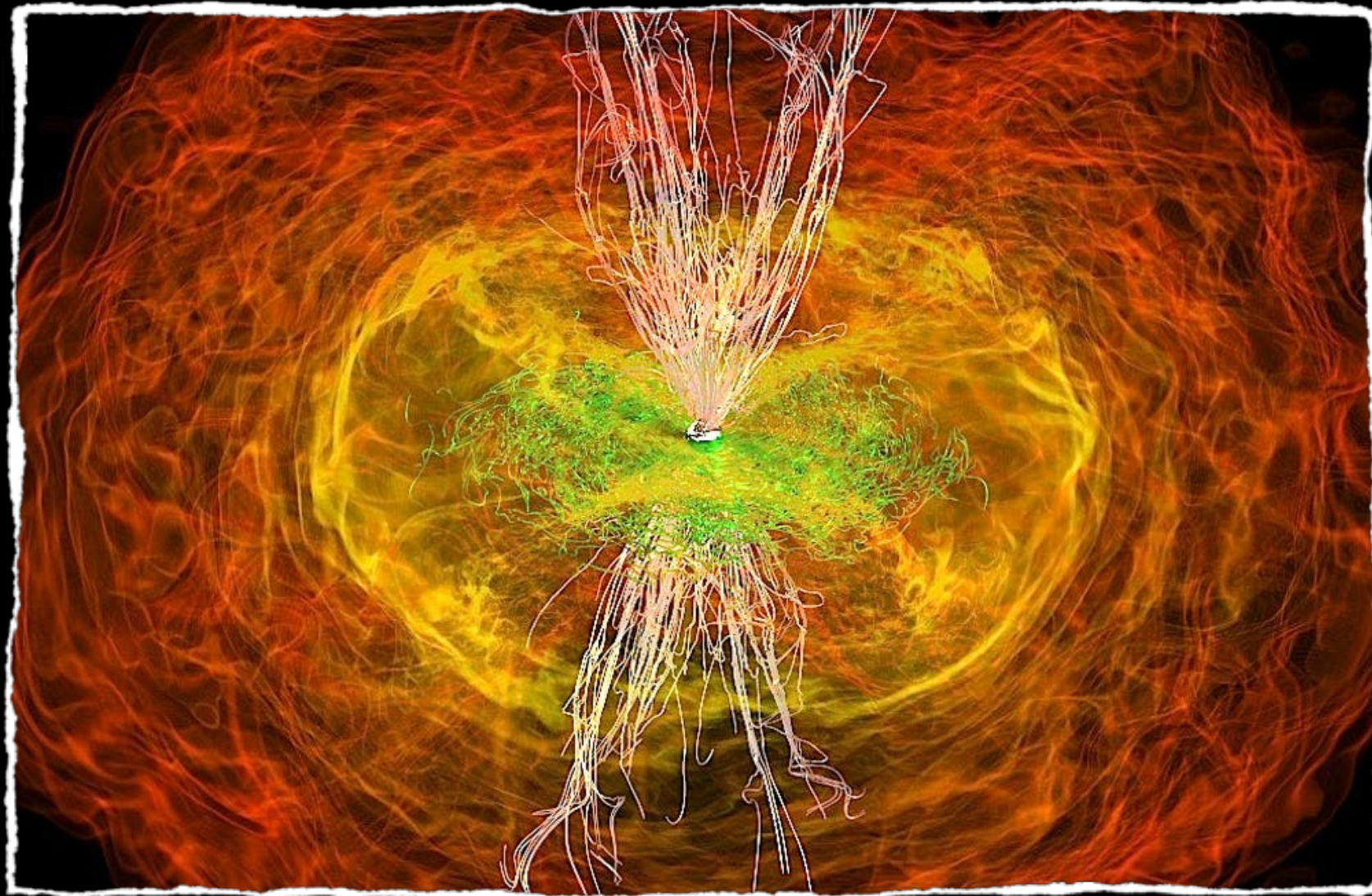
A spectroscopic approach to the EOS

- **Universal behaviour** and analytic modelling of post-merger relates position of these peaks with the EOS.
- Observation of the post-merger signal would constrain significantly the stellar radius; given **N detections**.



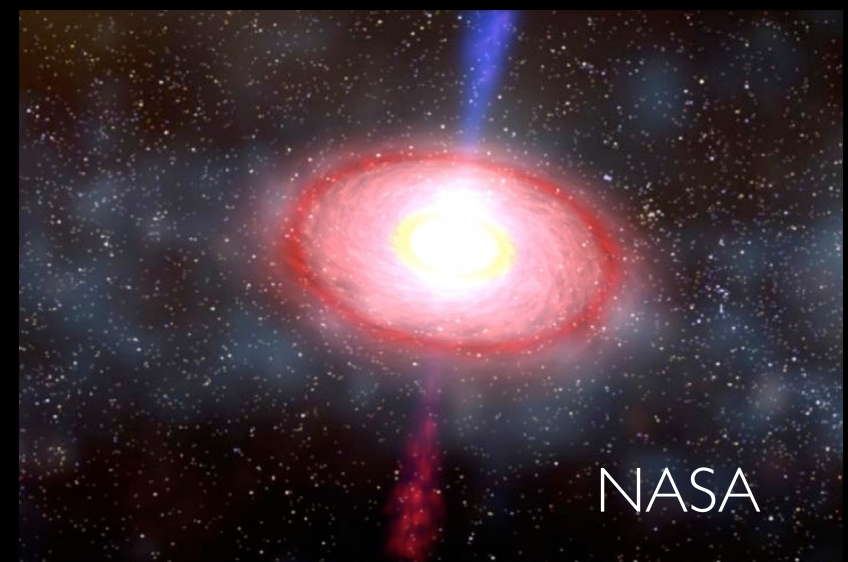
- discriminating stiff/soft EOSs possible even with moderate **$N \sim 10$**
- stiff EOSs: $|\Delta R / \langle R \rangle| < 10\%$ for **$N \sim 20$**
- soft EOSs: $|\Delta R / \langle R \rangle| \sim 10\%$ for **$N \sim 50$**
- golden binary: **$\text{SNR} \sim 6$** at **30 Mpc**
 $|\Delta R / \langle R \rangle| \simeq 2\%$ at 90% confidence

Electromagnetic counterparts



Electromagnetic counterparts

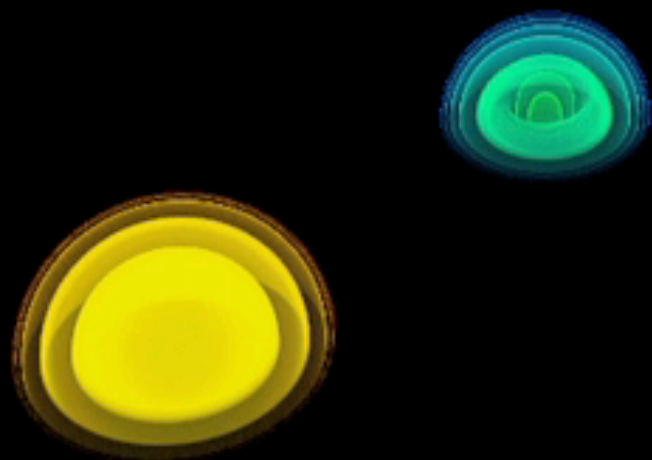
- Since 70's we have observed flashes of gamma rays with enormous energies 10^{50-53} erg: **gamma-ray bursts**.
- There are two families of bursts: “**long**” and “**short**”.
- The first ones last **tens** or more of **seconds** and could be due to the collapse of very massive stars.
- The second ones last **less** than a **second**.
- Merging neutron stars most reasonable explanation but how do you produce a **jet**?



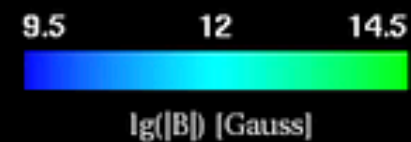
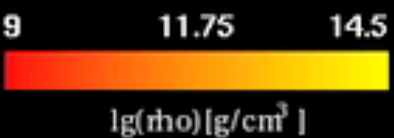
Presence of a jet immediately implies presence of large-scale magnetic fields

What happens when magnetised stars collide?

Need to solve equations of magnetohydrodynamics in addition to the Einstein equations

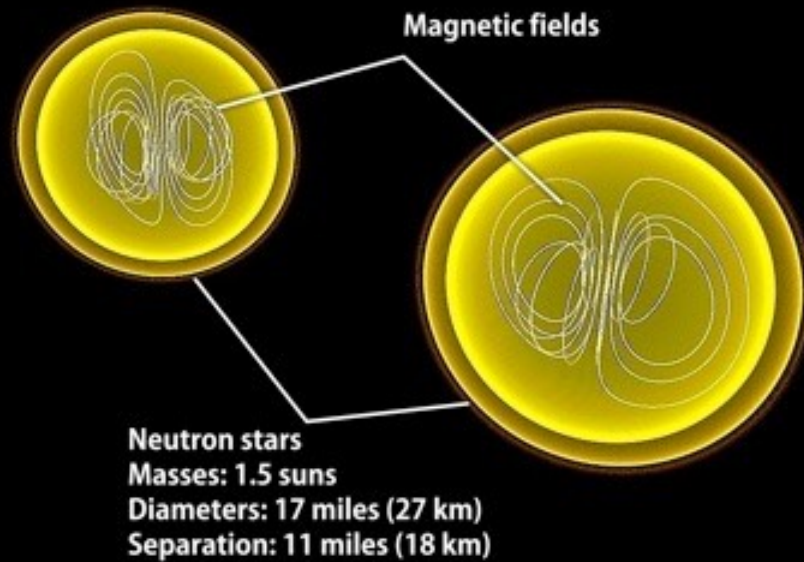


$$M = 1.5 M_{\odot}, B_0 = 10^{12} \text{ G}$$

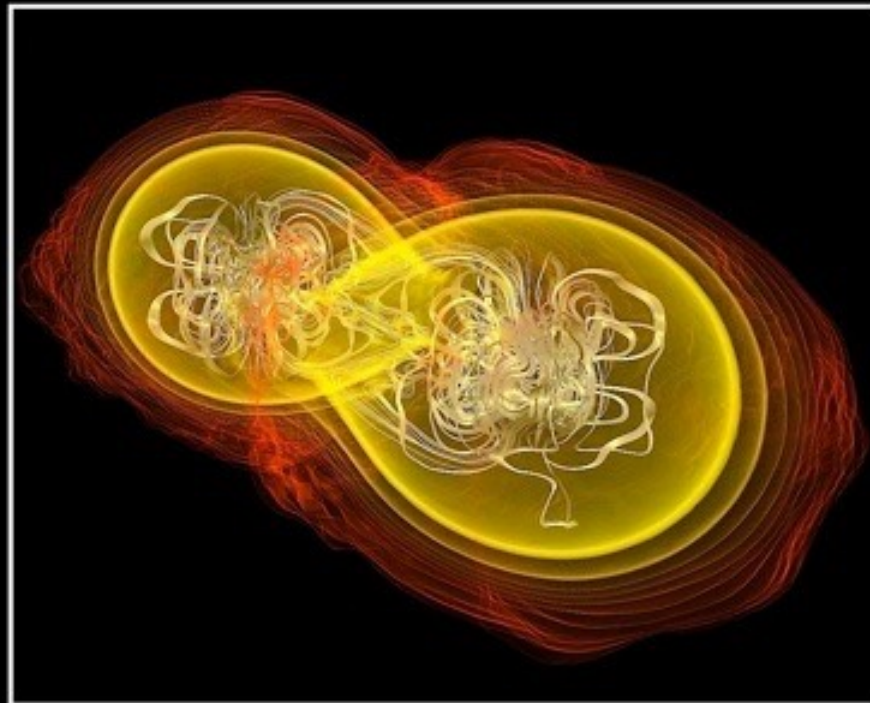


Animations:, LR, Koppitz

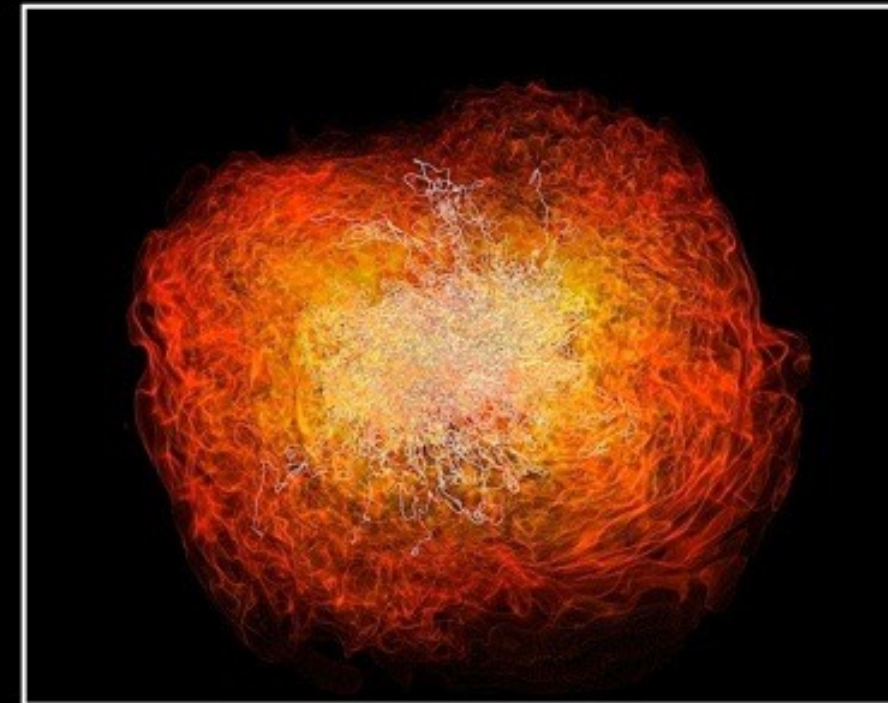
What happens when magnetised stars collide?



Simulation begins

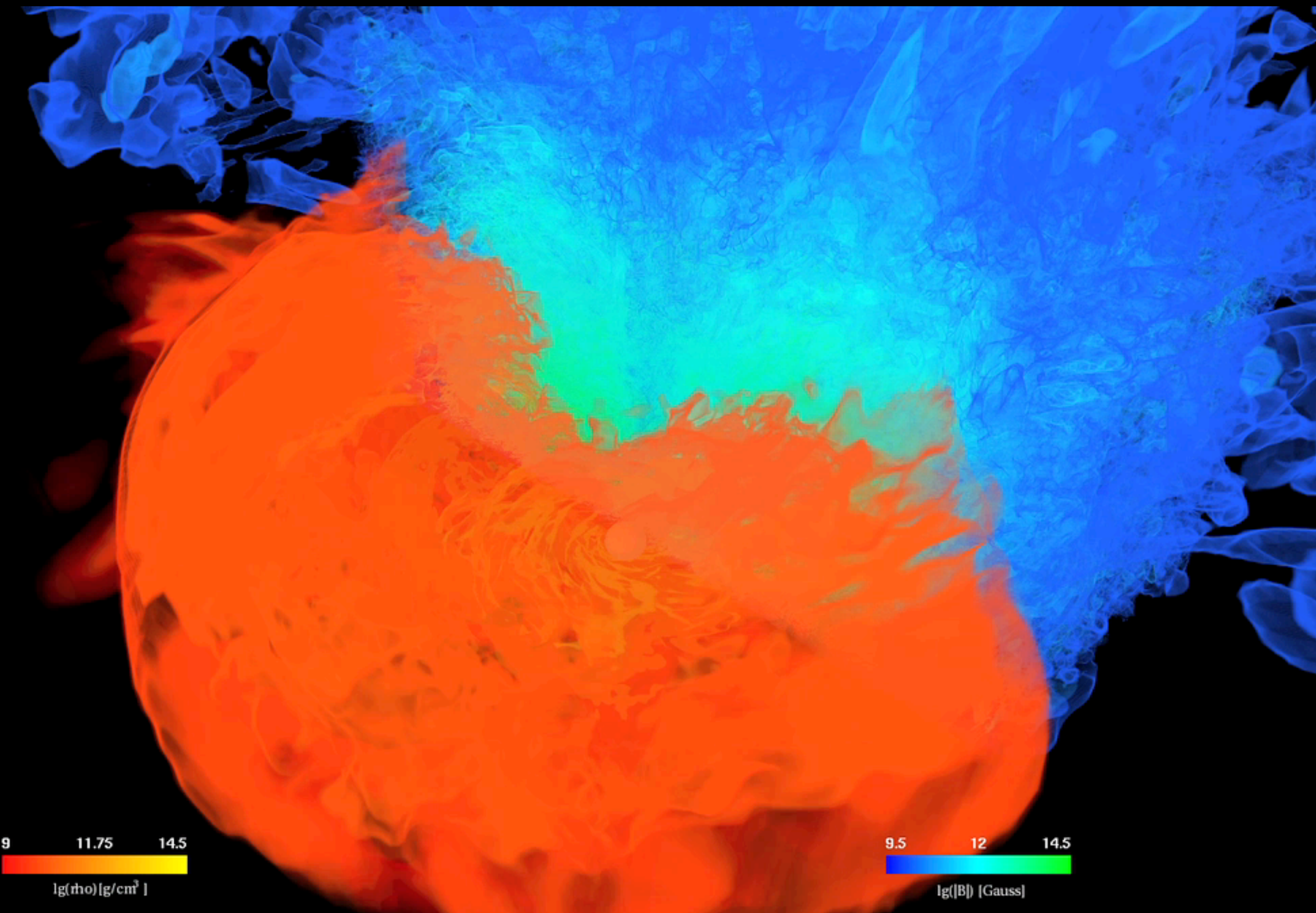


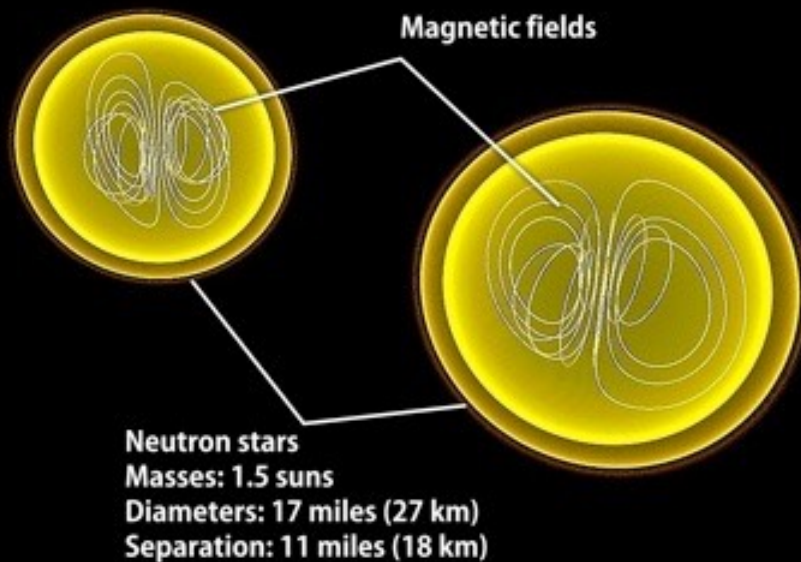
7.4 milliseconds



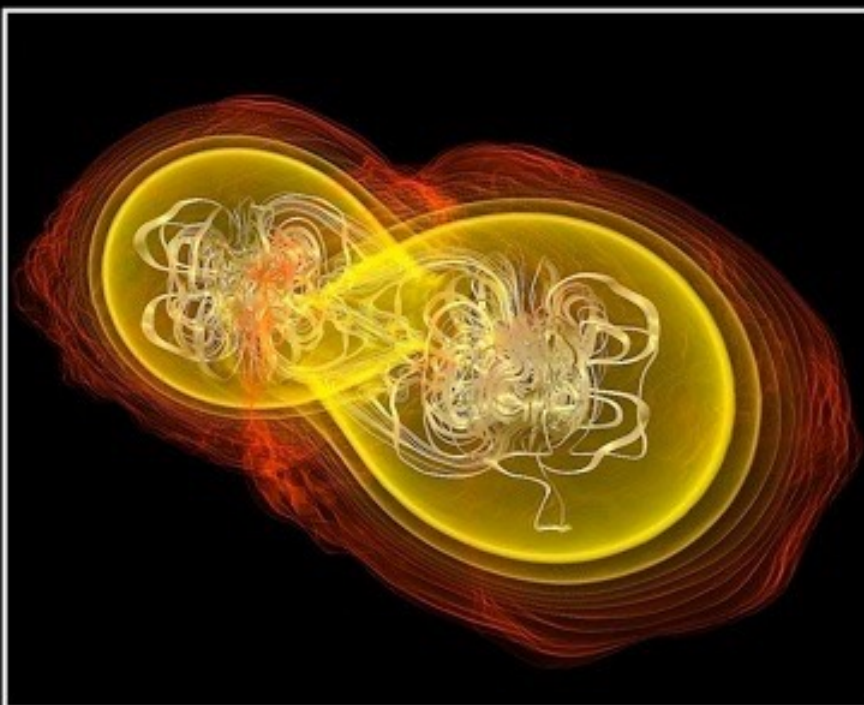
13.8 milliseconds

Magnetic fields in the HMNS have complex topology: dipolar fields are destroyed.

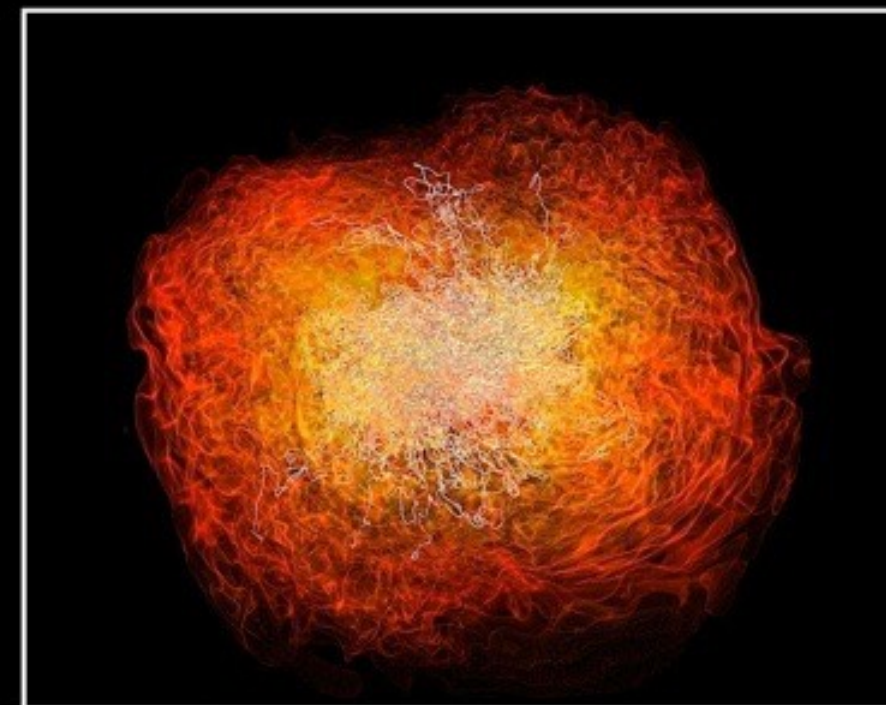




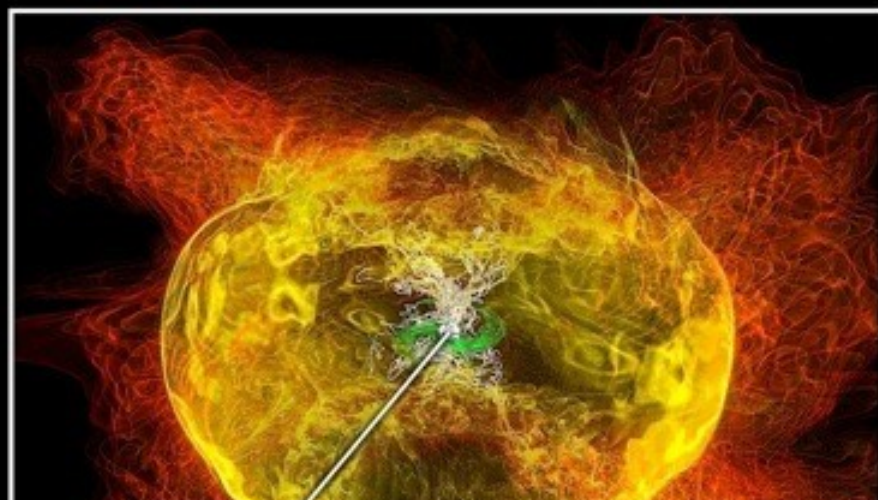
Simulation begins



7.4 milliseconds



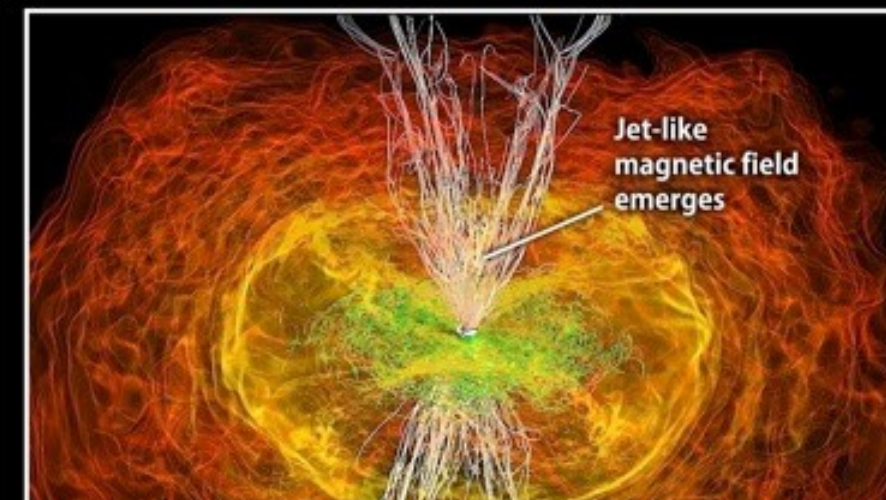
13.8 milliseconds



Black hole forms
Mass: 2.9 suns
Horizon diameter: 5.6 miles (9 km)



16.2 milliseconds



16.2 milliseconds

These simulations have shown that the merger of a magnetised binary has all the basic features behind SGRBs

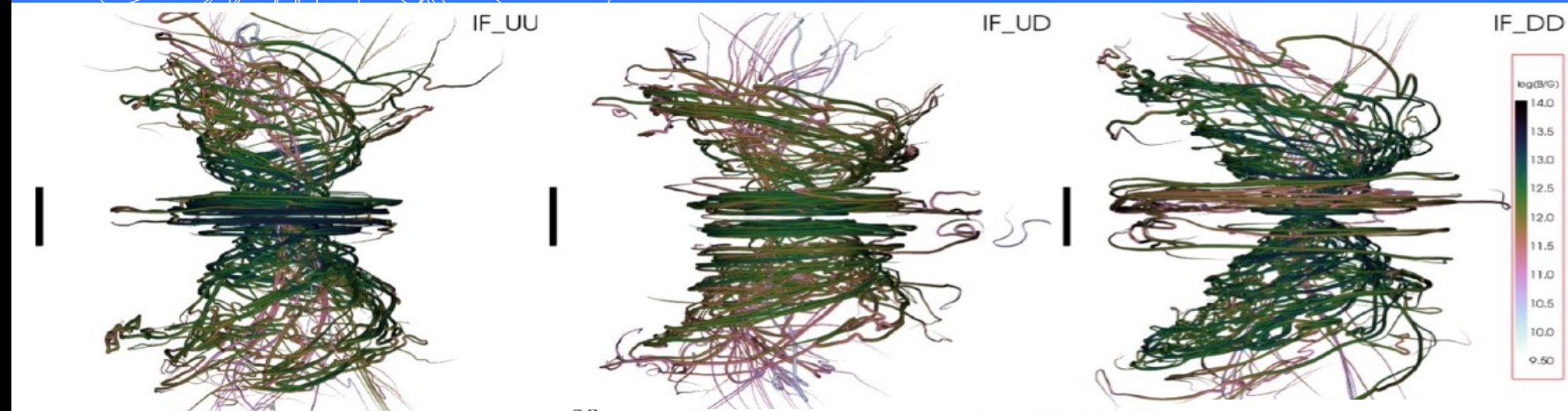
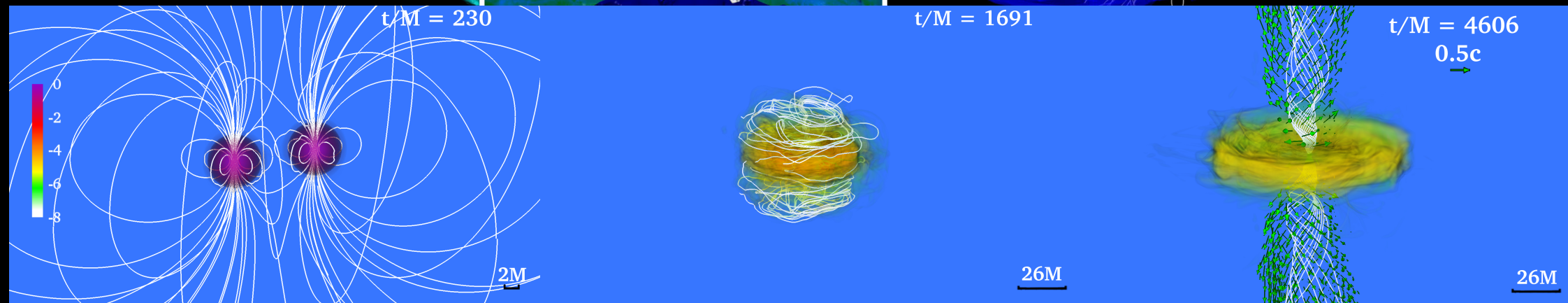
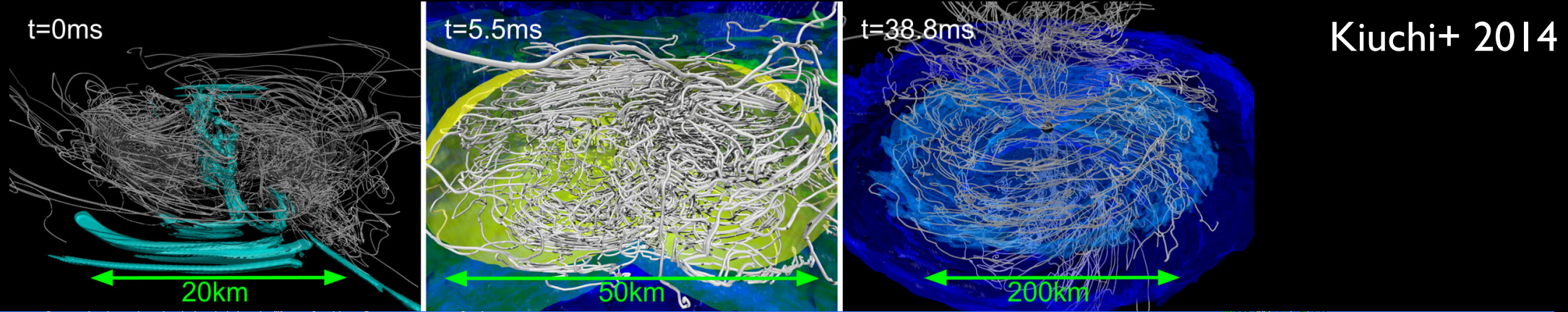
Credit: NASA/AEI/ZIB/M. Köppitz and L. Rezzolla

$$J/M^2 = 0.83$$

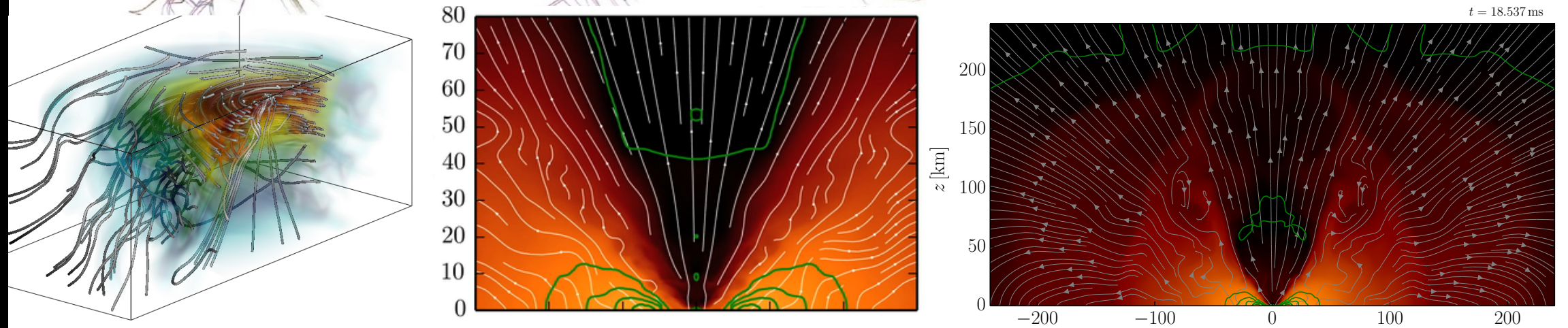
$$M_{\text{tor}} = 0.063 M_{\odot}$$

$$t_{\text{accr}} \simeq M_{\text{tor}}/\dot{M} \simeq 0.3 \text{ s}$$

With due differences, other groups confirm this picture



Kawamura+2016

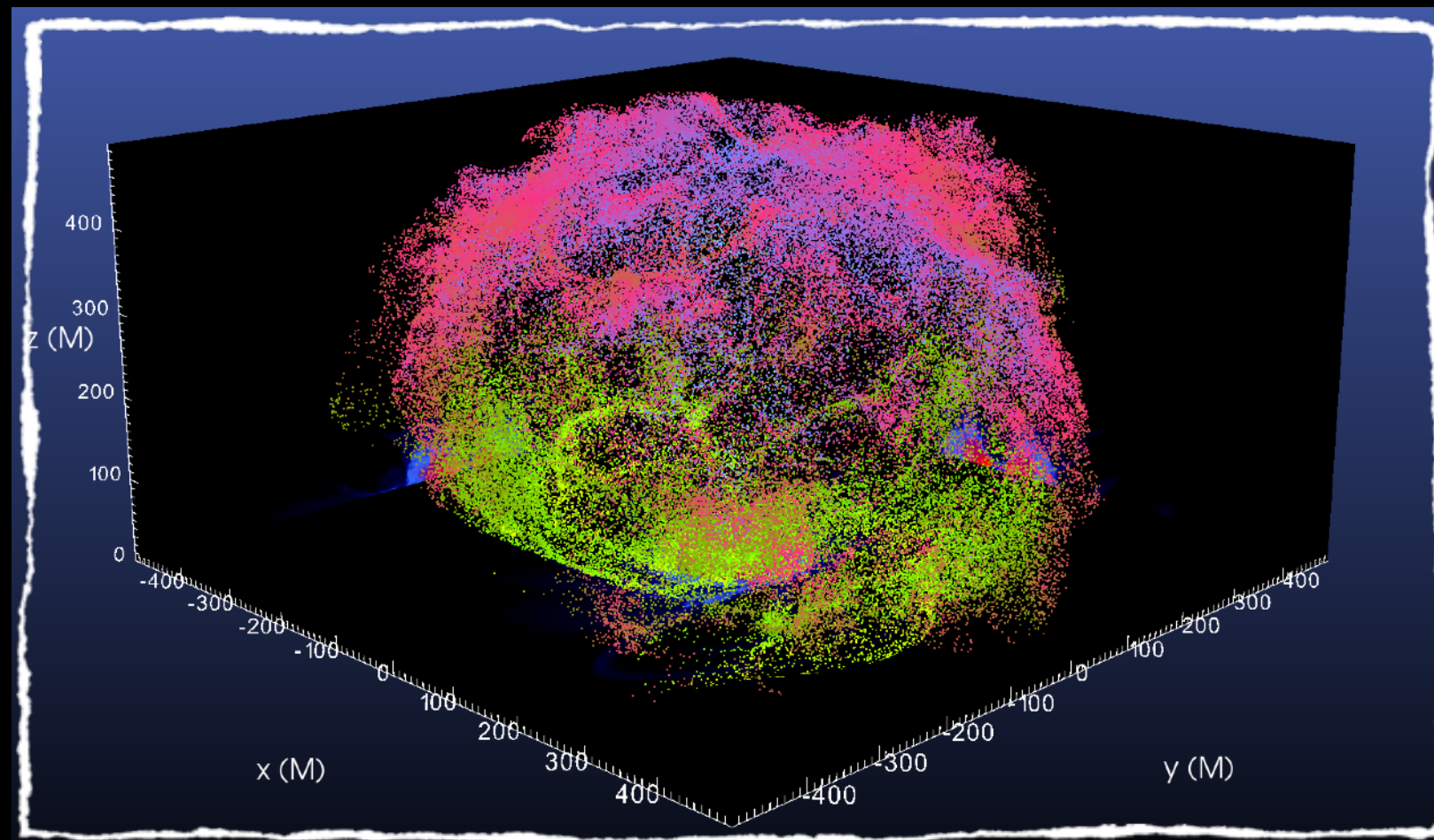


Dionysopoulou+ 2015



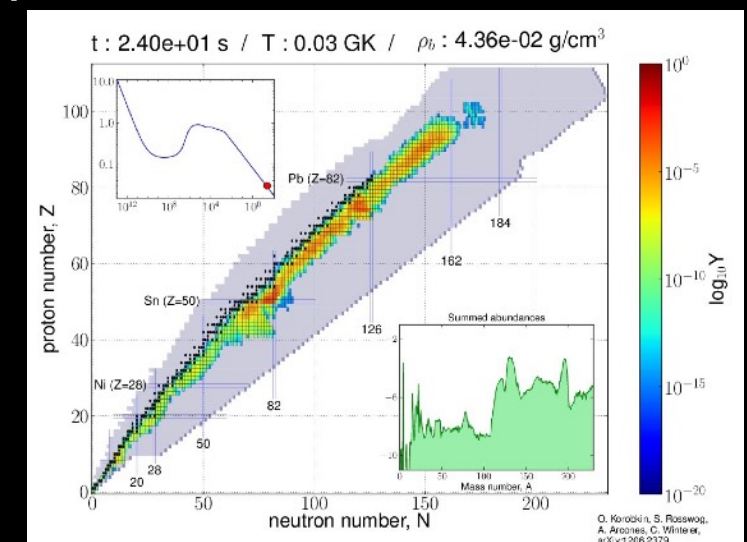
Ejected matter and nucleosynthesis

Bovard+ (2017)

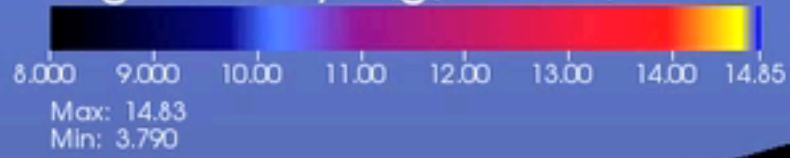


Nucleosynthesis

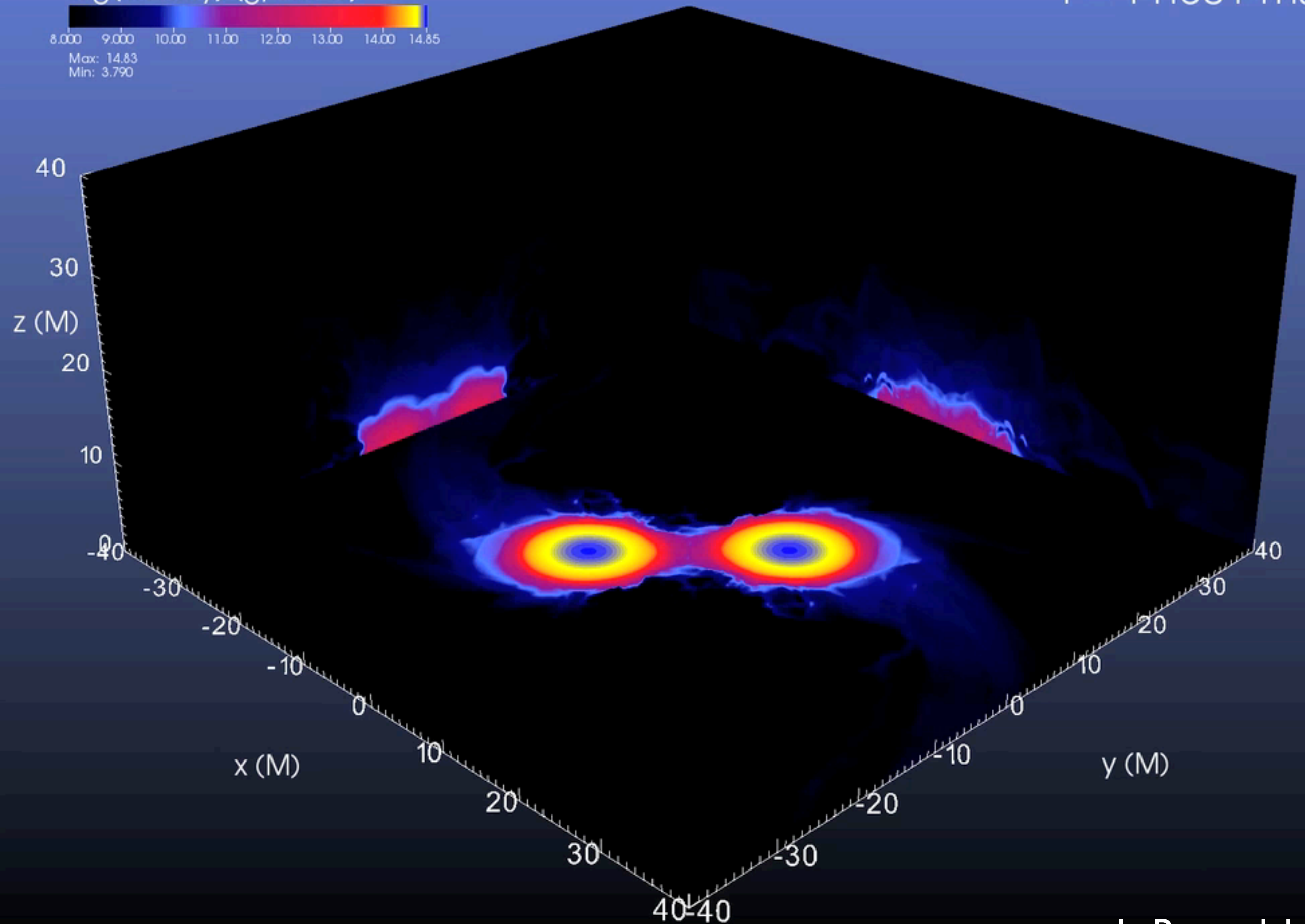
- Already in the 50's, nuclear physicists had tracked the production of elements in stars via nuclear fusion.
- **Heavy elements** ($A > 56$) cannot be produced in stellar interiors but can be synthesised during a **supernova**.
- SN simulations have shown that temperatures/energies not enough to produce “**very heavy**” elements ($A > 120$).
- To produce such elements very high temperatures and “**neutron-rich**” material is needed.
- **Neutron-star mergers** seem perfect candidates for this process!



log(density) (g/cm³)



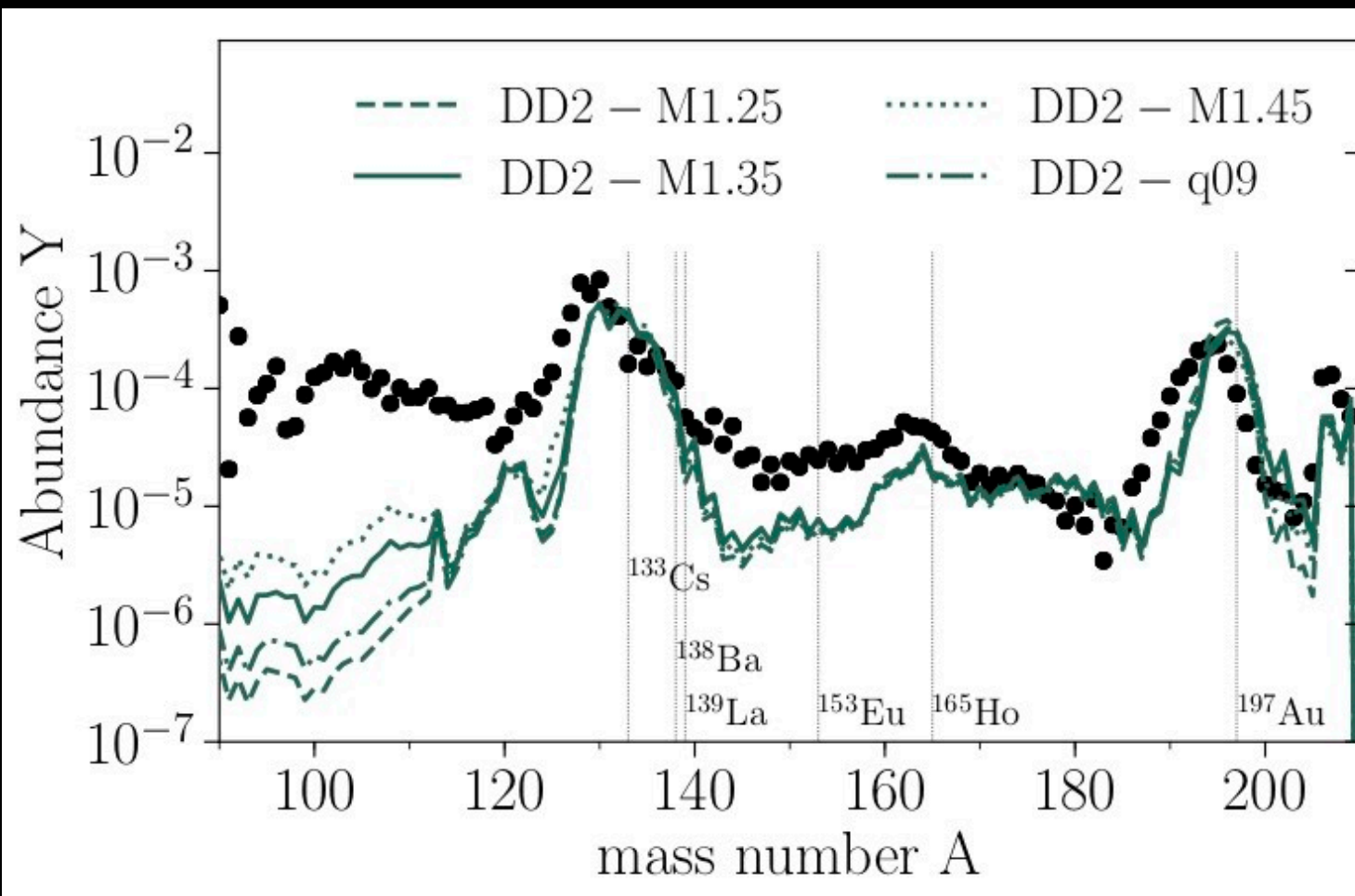
$t = 11.801$ ms



L. Bovard, LR

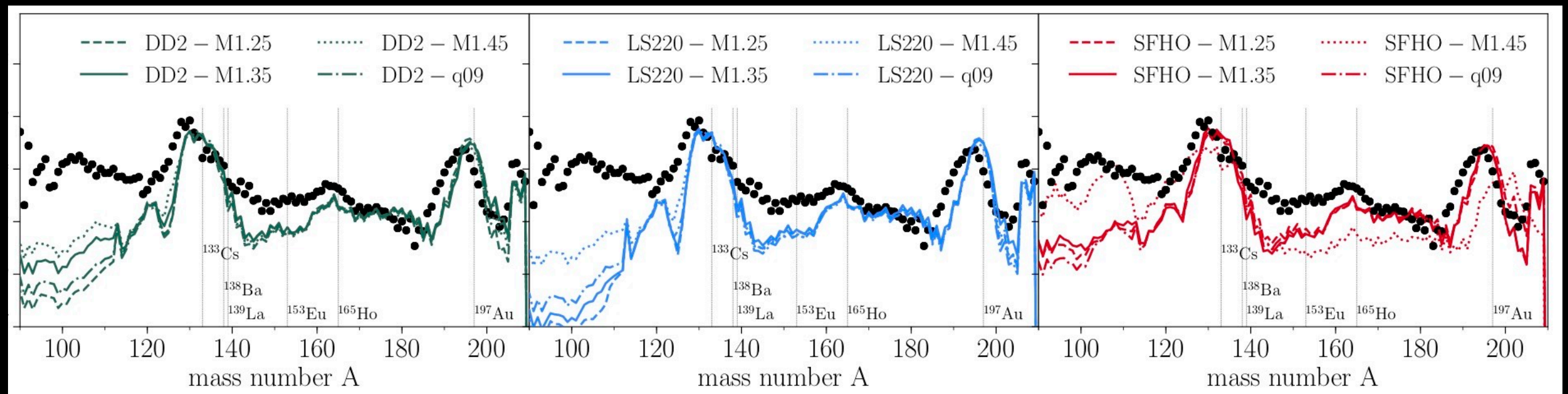
Relative abundances

- Mass ejection can either be **dynamical** (shocks; 100 ms) or **secular** (magnetic or neutrino-driven winds; 1-10 s).
- Even **tiny amounts** of ejected matter ($0.01 M_{\odot}$) sufficient to explain observed abundances.
- Abundances for $A > 120$ good agreement with solar. **robust** for different **EOSs**, masses, nuclear reactions and merger type



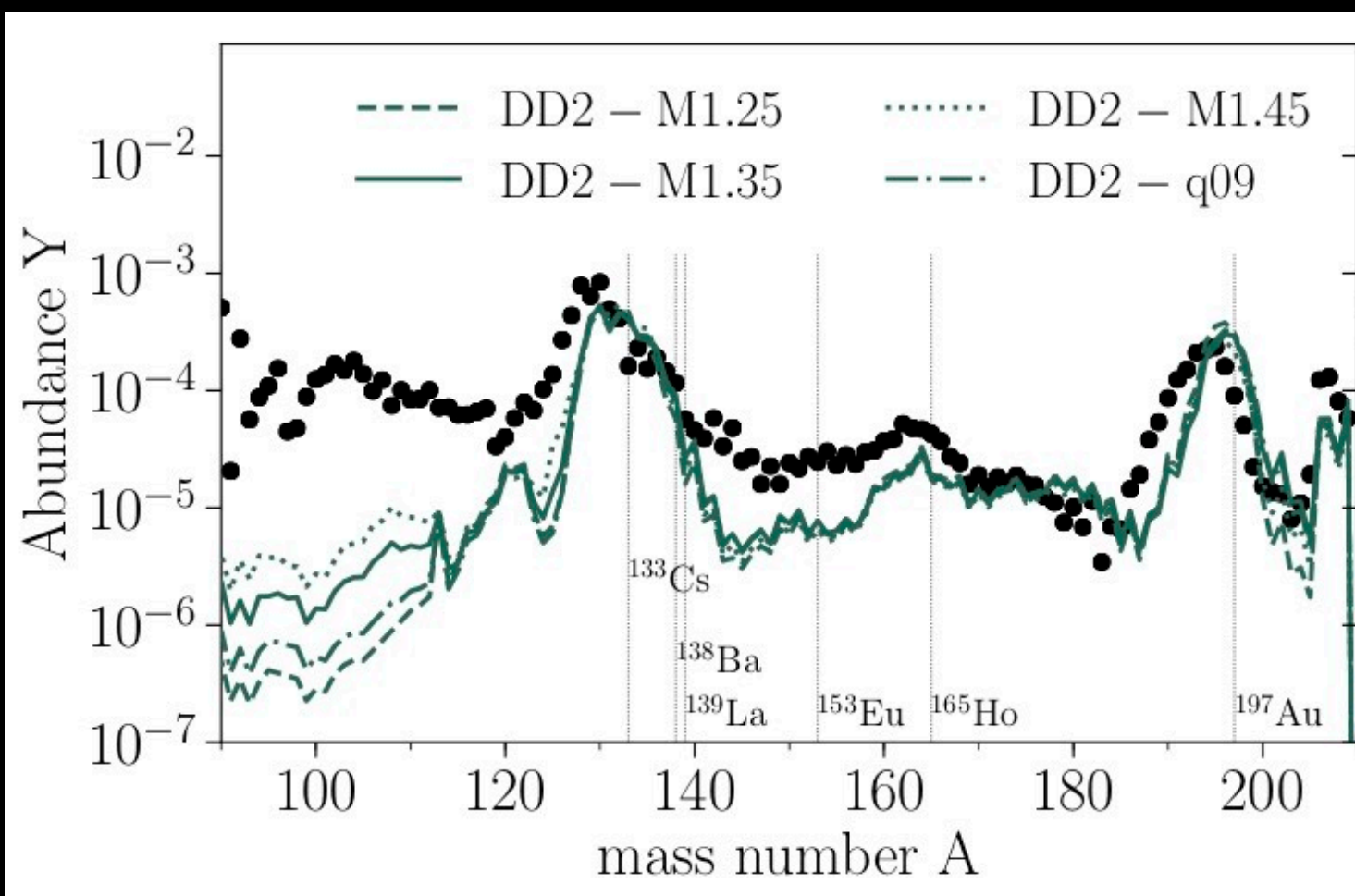
Relative abundances

- Mass ejection can either be **dynamical** (shocks; 100 ms) or **secular** (magnetic or neutrino-driven winds; 1-10 s).
- Even **tiny amounts** of ejected matter ($0.01 M_{\odot}$) sufficient to explain observed abundances.
- Abundances for $A > 120$ good agreement with solar. **robust** for different **EOSs**, masses, nuclear reactions and merger type



Relative abundances

- Mass ejection can either be **dynamical** (shocks; 100 ms) or **secular** (magnetic or neutrino-driven winds; 1-10 s).
- Even **tiny amounts** of ejected matter ($0.01 M_{\odot}$) sufficient to explain observed abundances.
- Abundances for $A > 120$ good agreement with solar. **robust** for different **EOSs, masses, nuclear reactions and merger type**



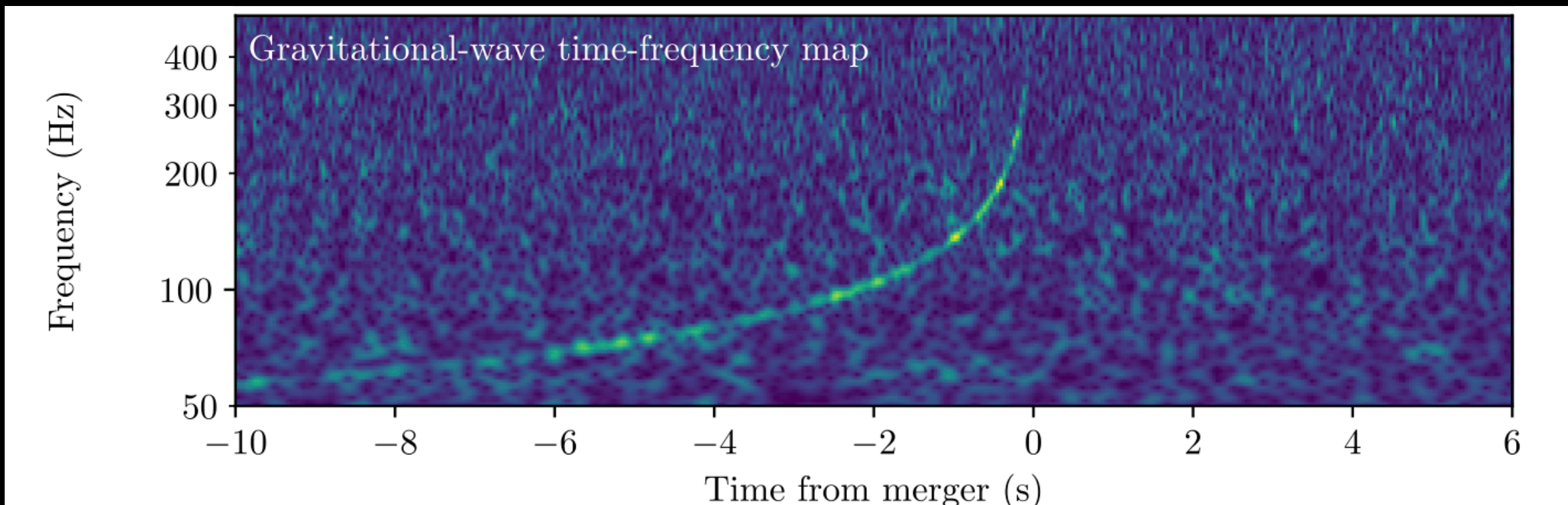
- GW170817 produced total of **16,000** times the mass of the Earth in heavy elements (**10** Earth masses in **gold/platinum**)
- We are not only **stellar dust** but also **neutron-star dust!**

GW170817, maximum mass, radii and tidal deformabilities

LR, Most, Weih, ApJL (2018)

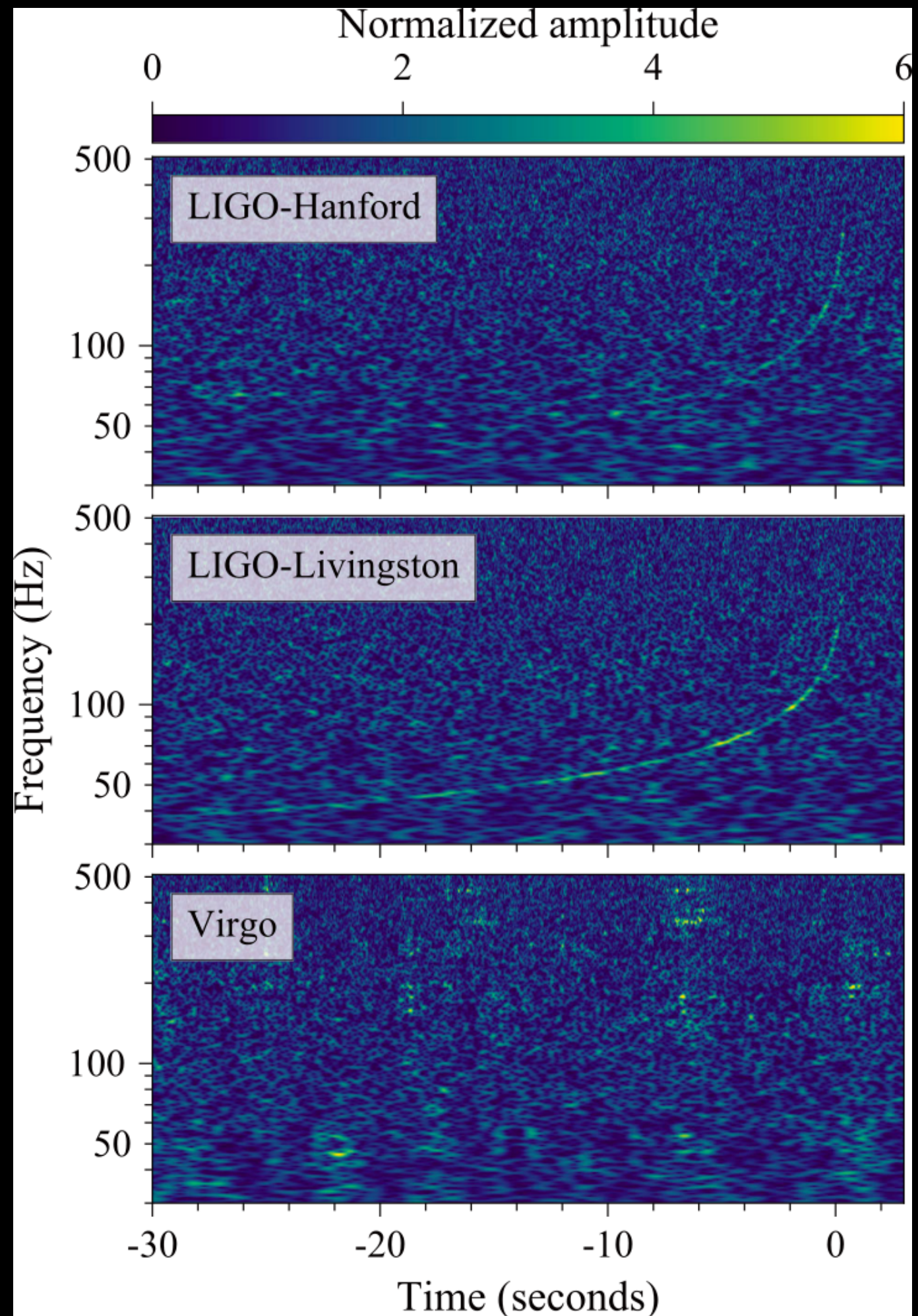
Most, Weih, LR, Schaffner-Bielich, PRL (2018)

Köppel, Bovard, LR, ApJL (2018)



GW170817: the first binary neutron-star system

- * Unfortunately only the **inspiral** signal was detected.
- * Fortunately this was **sufficient** to set a number of constraints on max. mass, tidal deformability, radii, etc.

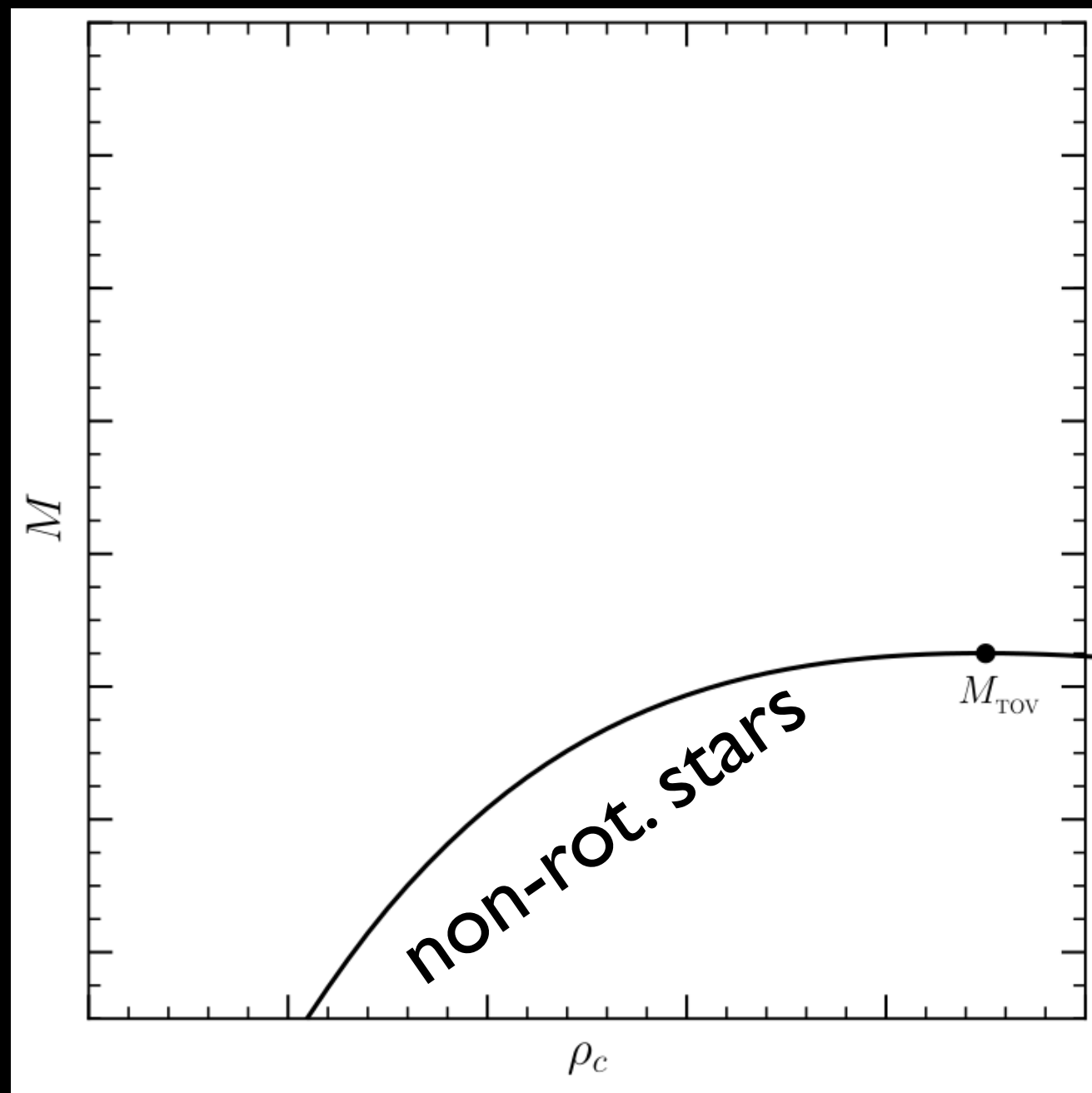


Limits on the maximum mass

- The remnant of GW170817 was a hypermassive star, i.e. a differentially rotating object with initial **gravitational** mass:

$$M_1 + M_2 = 2.74_{-0.01}^{+0.04} M_{\odot}$$

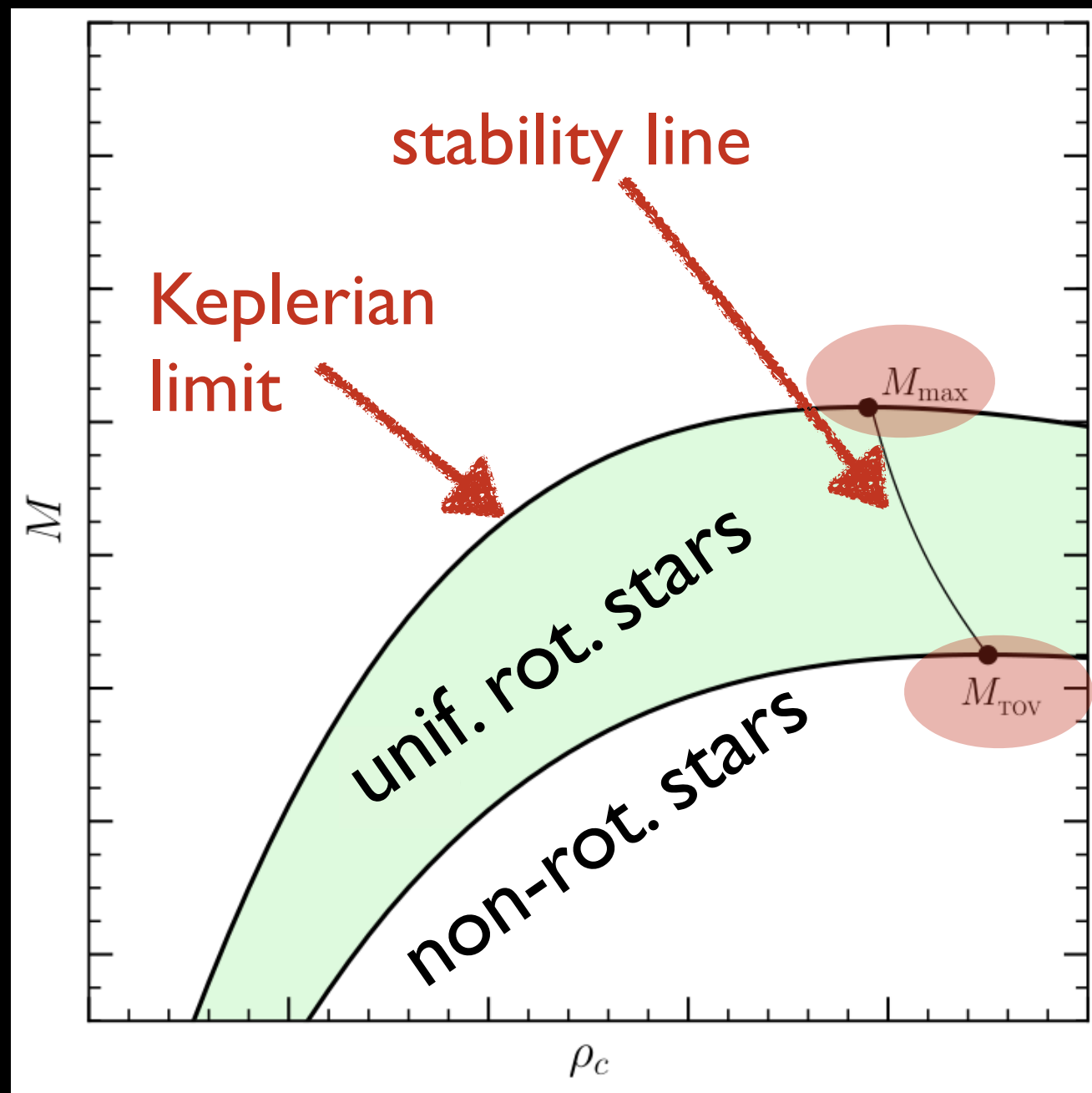
- Sequences of equilibrium models of **nonrotating** stars will have a maximum mass: M_{TOV}



Limits on the maximum mass

- The remnant of GW170817 was a hypermassive star, i.e. a differentially rotating object with initial **gravitational** mass:

$$M_1 + M_2 = 2.74_{-0.01}^{+0.04} M_{\odot}$$



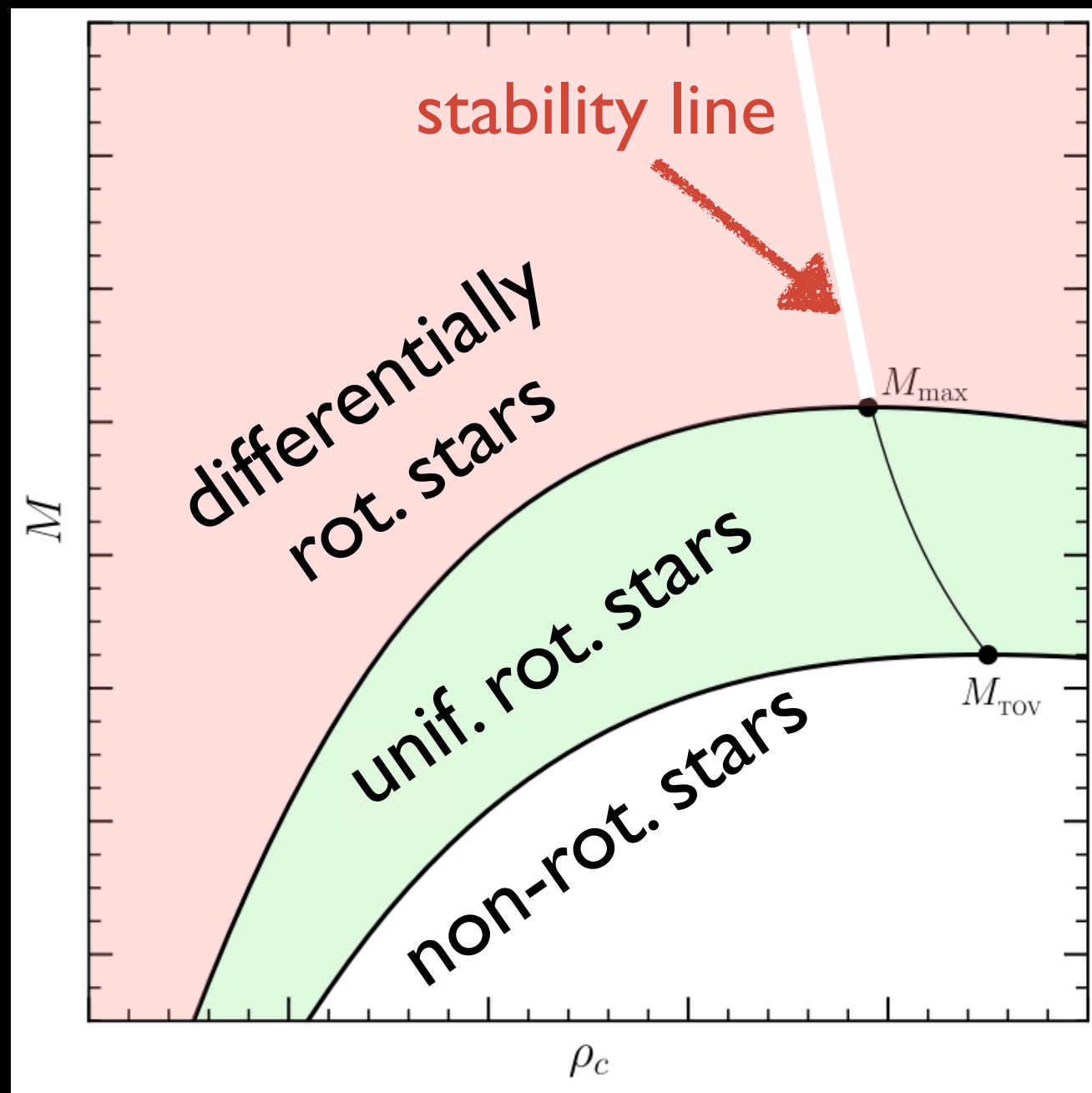
- Sequences of equilibrium models of **nonrotating** stars will have a maximum mass: M_{TOV}
- This is true also for **uniformly** rotating stars at mass shedding limit: M_{max}
- M_{max} simple and **quasi-universal** function of M_{TOV} (Breu & LR 2016)

$$M_{\text{max}} = 1.20_{-0.05}^{+0.02} M_{\odot}$$

Limits on the maximum mass

- The remnant of GW170817 was a hypermassive star, i.e. a differentially rotating object with initial **gravitational** mass:

$$M_1 + M_2 = 2.74_{-0.01}^{+0.04} M_{\odot}$$

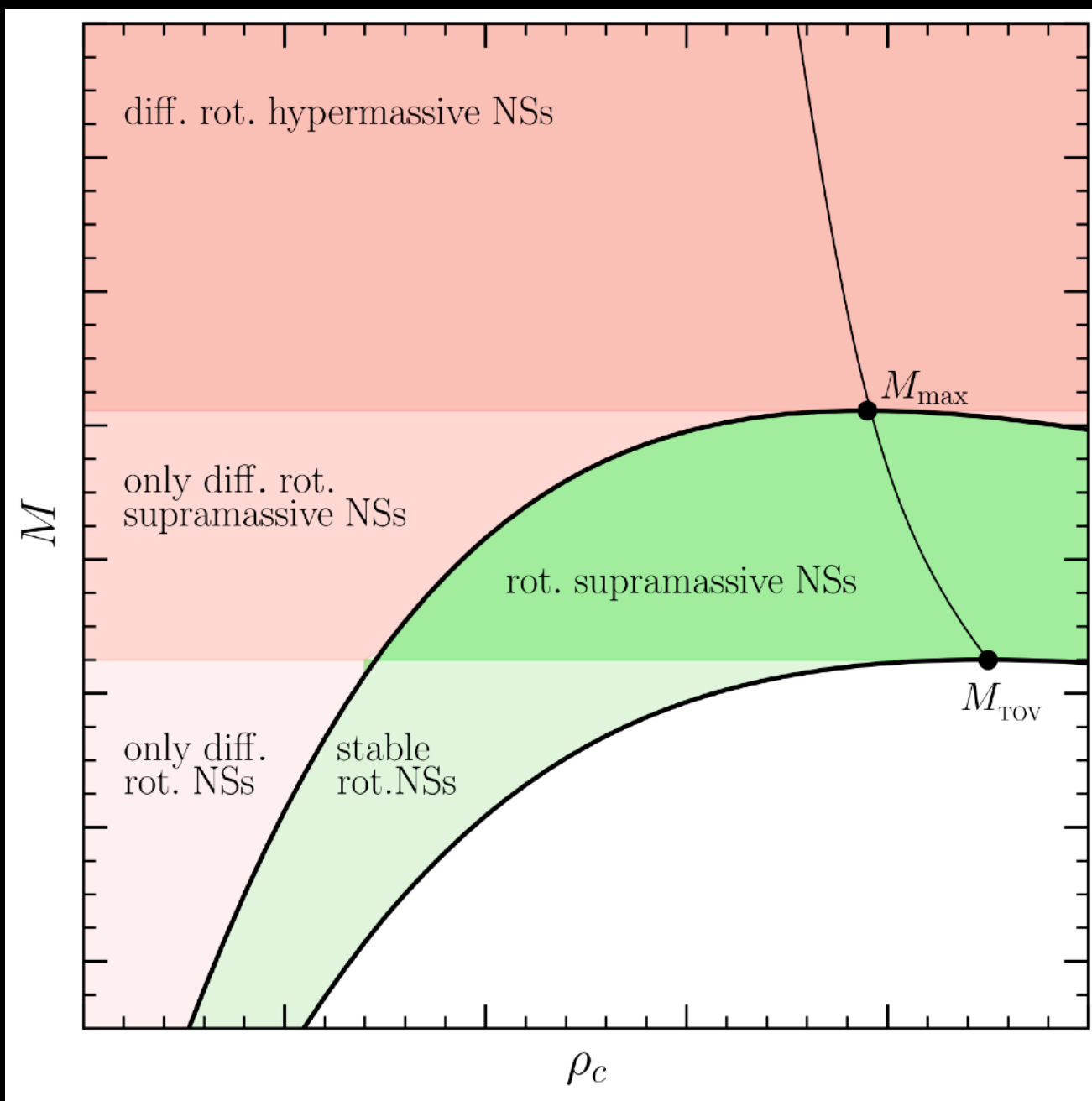


- Green** region is for **uniformly** rotating equilibrium models.
- Salmon** region is for **differentially** rotating equilibrium models.
- Stability line** is simply extended in larger space (Weih+18)

Limits on the maximum mass

- The remnant of GW170817 was a hypermassive star, i.e. a differentially rotating object with initial **gravitational** mass:

$$M_1 + M_2 = 2.74^{+0.04}_{-0.01} M_{\odot}$$



- Green** region is for **uniformly** rotating equilibrium models.
- Salmon** region is for **differentially** rotating equilibrium models.

- Supramassive** stars have:

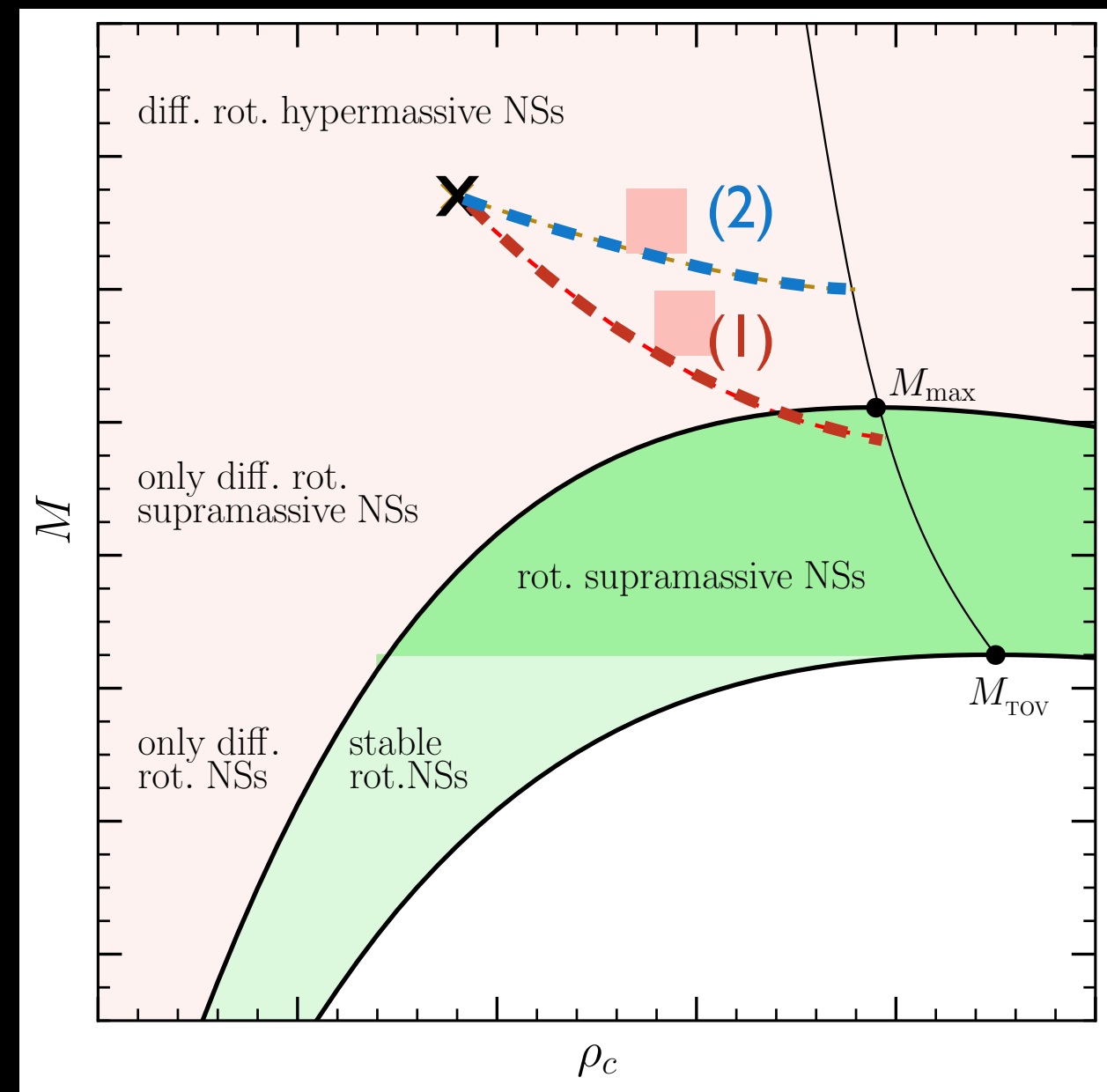
$$M > M_{\text{TOV}}$$

- Hypermassive** stars have:

$$M > M_{\text{max}}$$

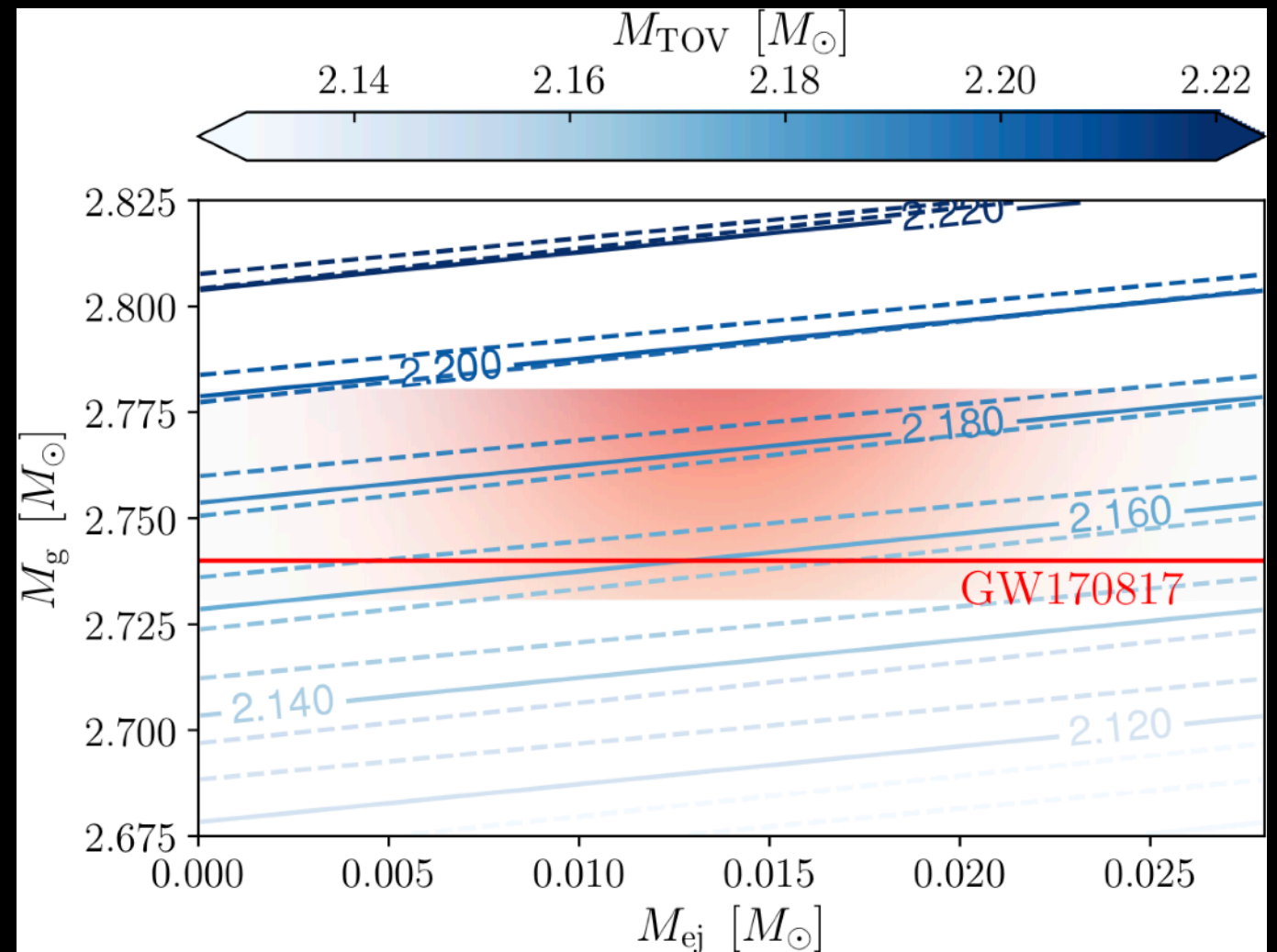
Limits on the maximum mass

- GW170817 produced object "X"; GRB implies a BH has been formed: "X" followed two possible tracks: **fast (2)** and **slow (1)**
- It rapidly produced a BH when still **differentially** rotating **(2)**
- It lost differential rotation leading to a **uniformly** rotating core **(1)**.
- **(1)** is much more likely because of large ejected mass (long lived).
- Final mass is near M_{\max} and we know this is universal!



let's recap...

- The merger product of GW170817 was initially **differentially** rotating but collapsed as **uniformly** rotating object.
- Use measured **gravitational** mass of GW170817
- Remove **rest mass** deduced from kilonova emission
- Use **universal relations** and account for errors to obtain



pulsar
timing

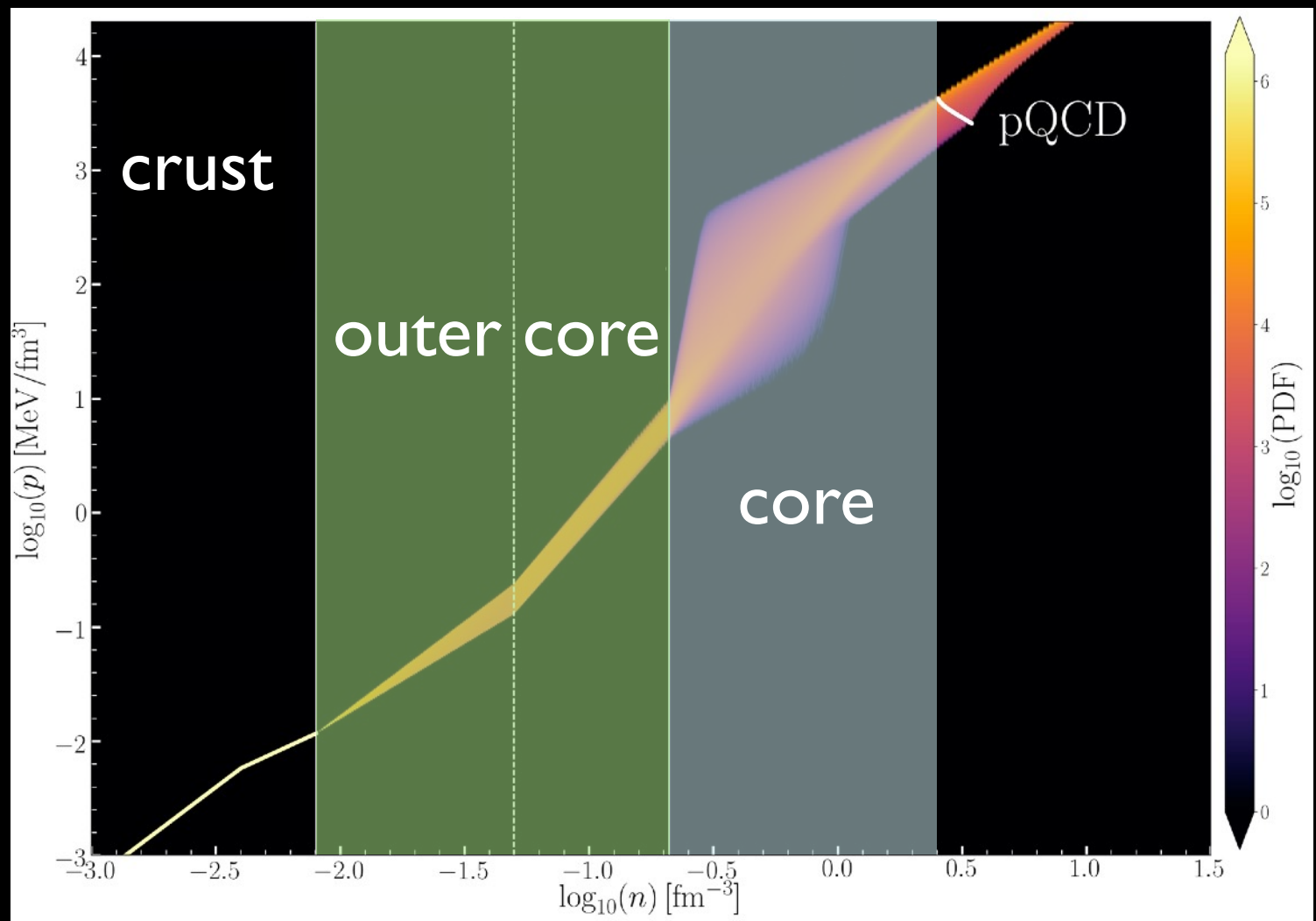
$$2.01^{+0.04}_{-0.04} \leq M_{\text{TOV}} / M_{\odot} \leq 2.16^{+0.17}_{-0.15}$$

universal relations
and GW170817;
similar estimates
by other groups

Limits on radii and deformabilities

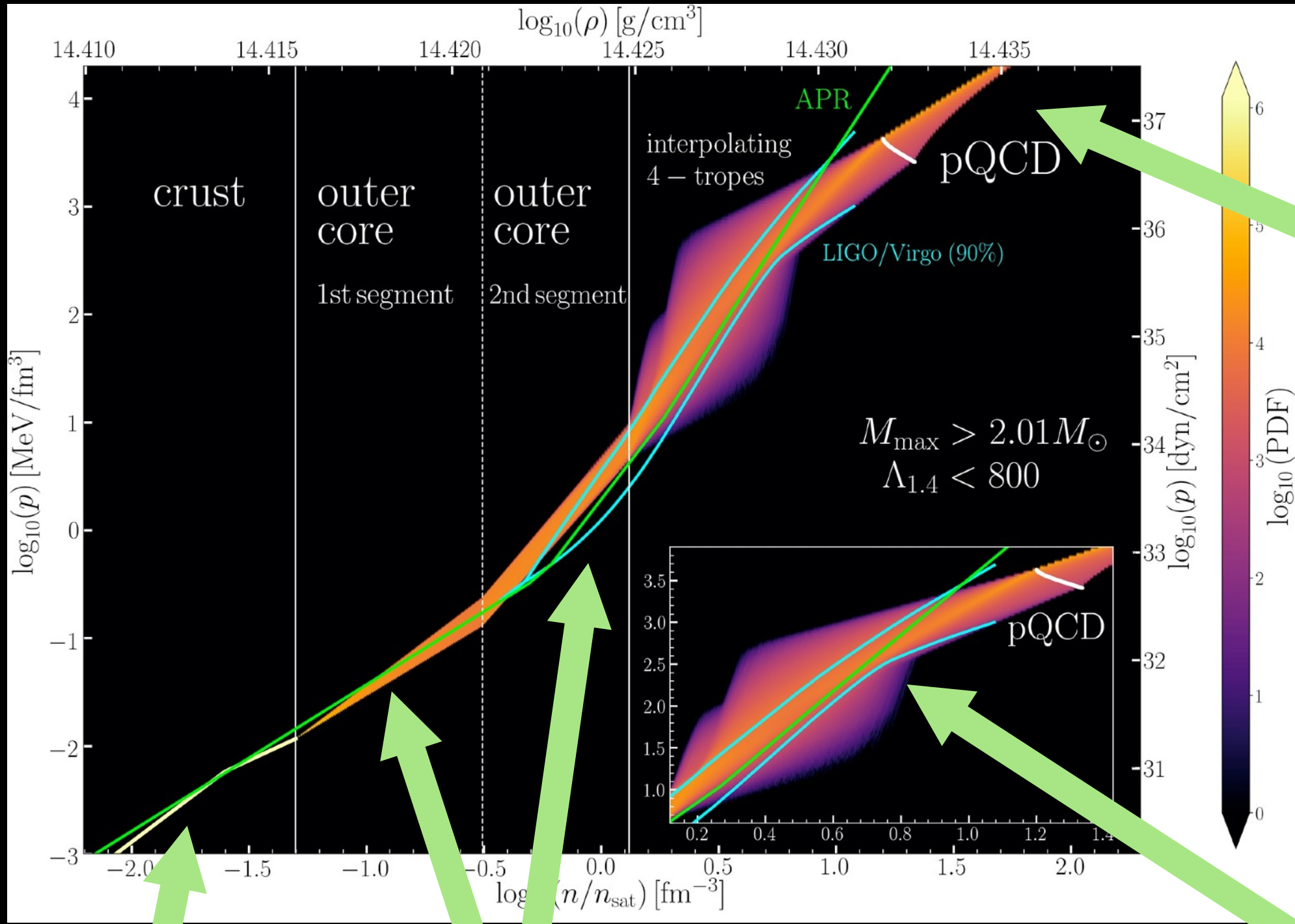
- Can new constraints be set on typical radius and tidal deformability by using GW170817?

- **Ignorance** can be parameterised and EOSs can be built arbitrarily as long as they satisfy specific **constraints** on **low** and **high** densities.



parametrising our ignorance

- Construct most generic family of NS-matter EOs



from $\mu_b = 2.6 \text{ GeV}$
NNLO pQCD
Kurkela+ (2014)
Fraga+ (2014)

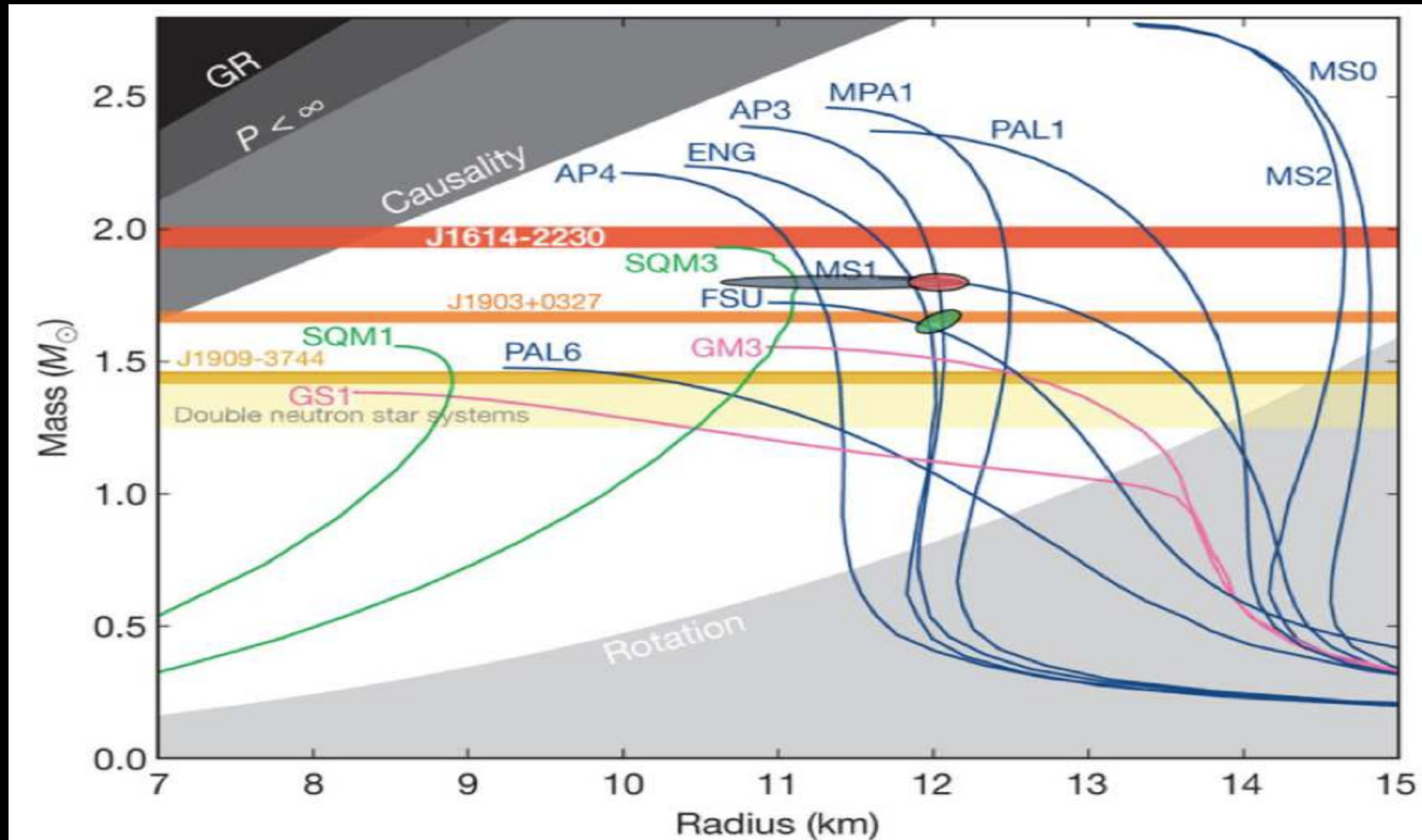
BPS

polytropic fit of Drischler+ (2016)
(large impact on results)

interpolation
by matching 4
polytropes

Mass-radius relations

- We have produced 10^6 EOSs with about 10^9 stellar models.
- Can impose differential constraints from the **maximum mass** and from the **tidal deformability** from **GW170817**

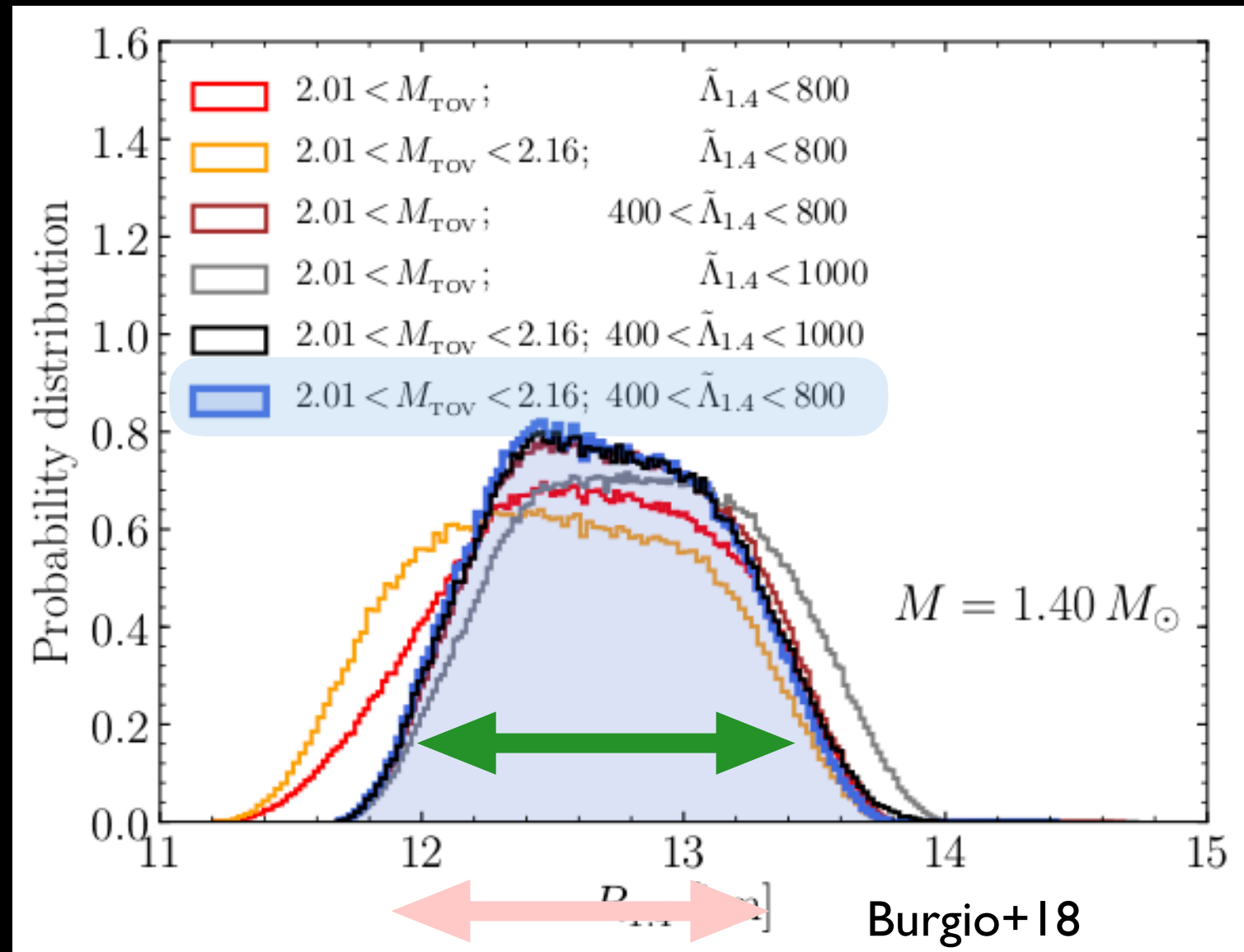


one-dimensional cuts

- Closer look at a mass of $M = 1.40 M_{\odot}$
- Can play with different constraints on maximum mass and tidal deformability.
- Overall distribution is very robust

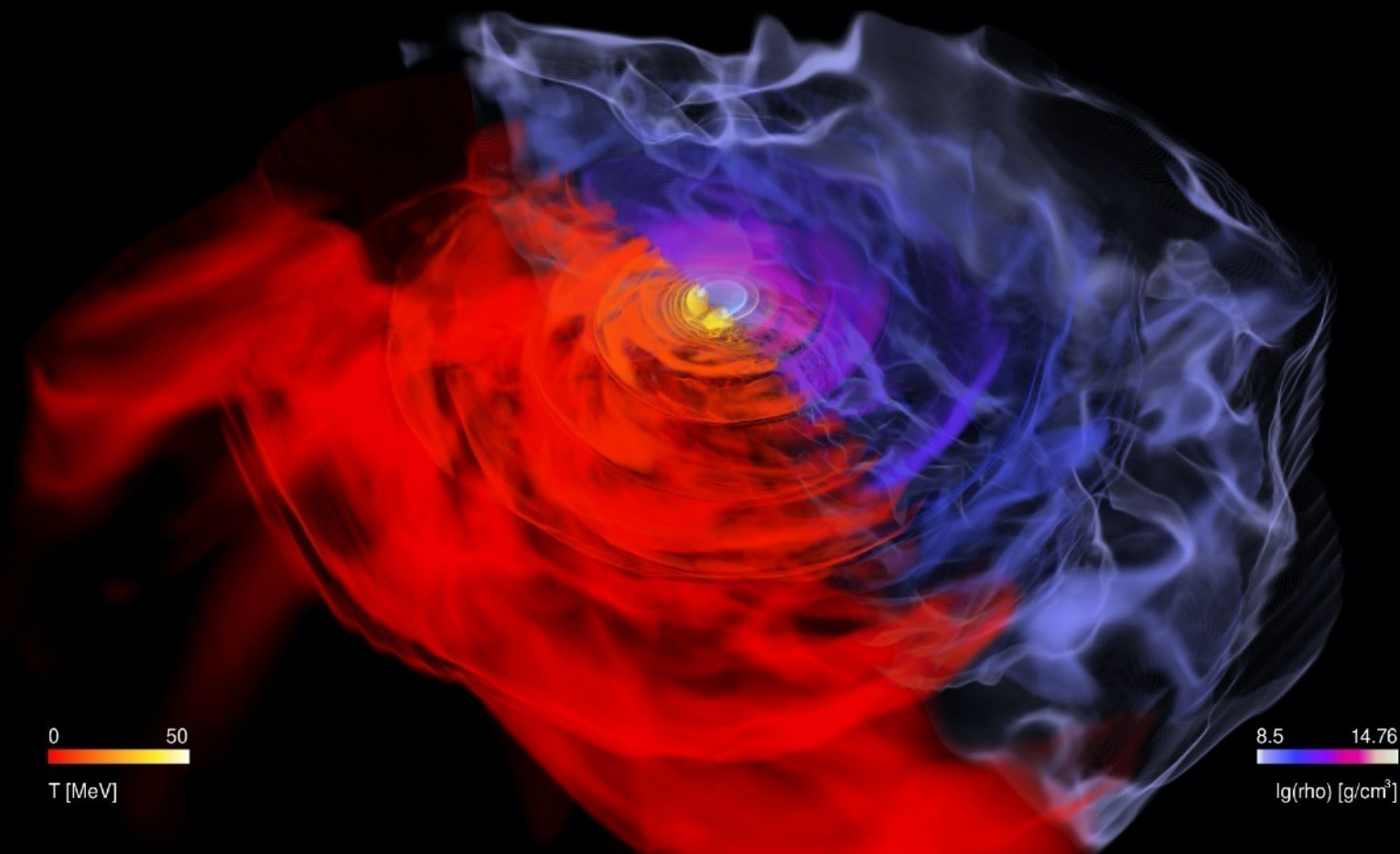
$$12.00 < R_{1.4}/\text{km} < 13.45$$

$$\langle R_{1.4} \rangle = 12.45 \text{ km}$$

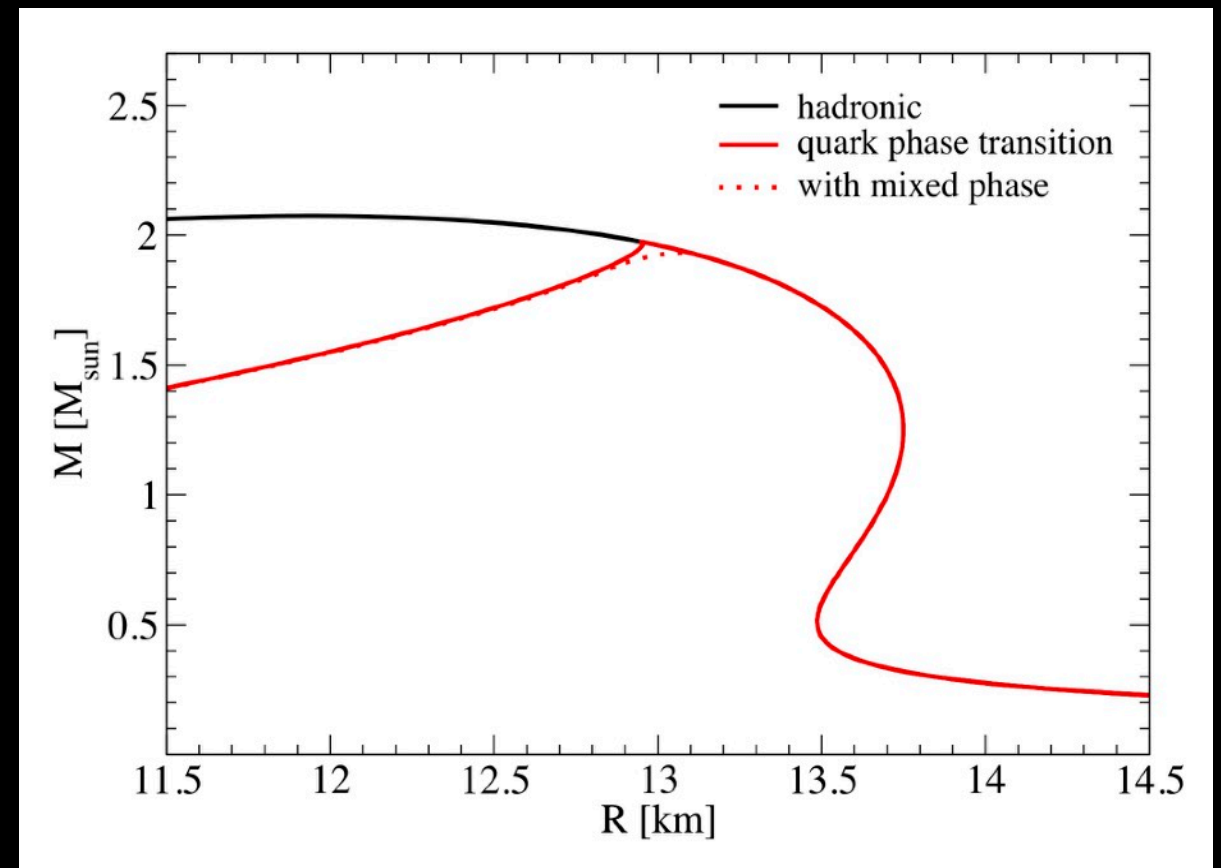
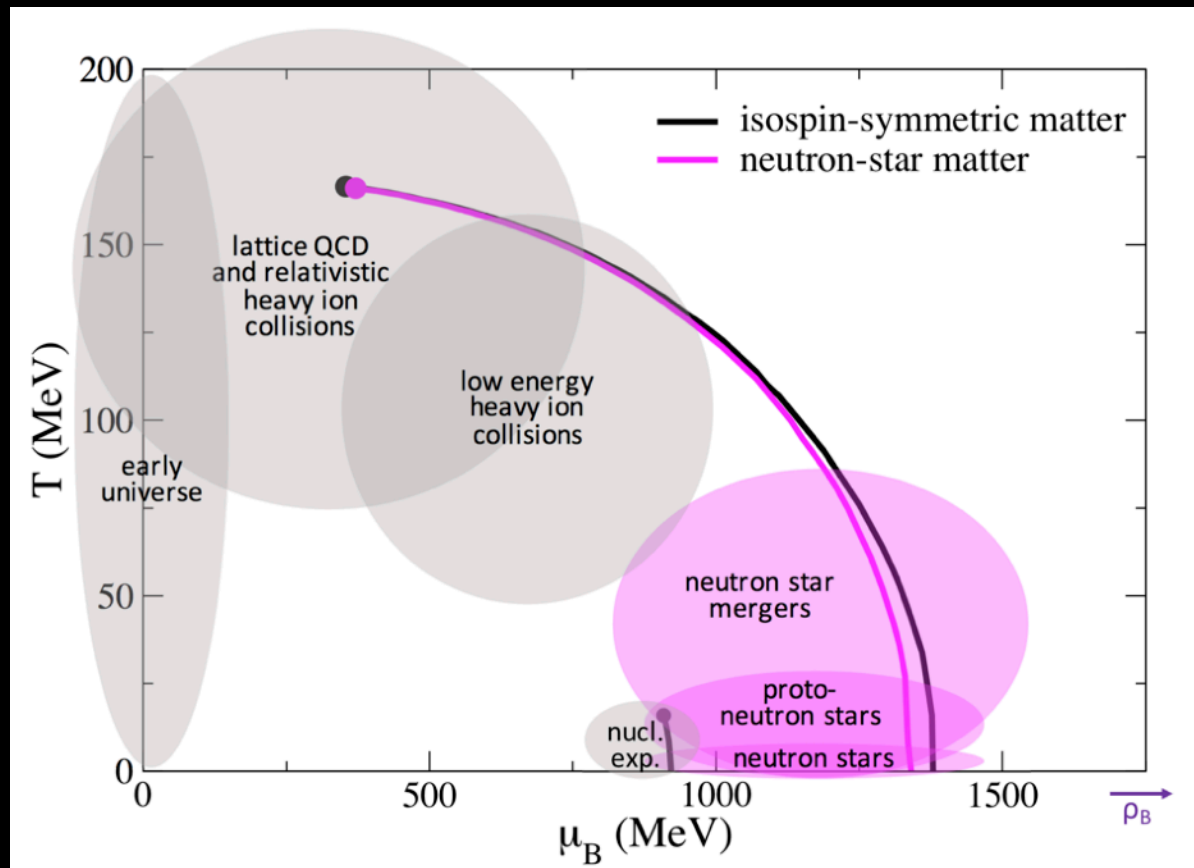


Phase transitions and their signatures

Most, Papenfort, Dexheimer, Hanauske, Schramm, Stoecker, LR (2019)

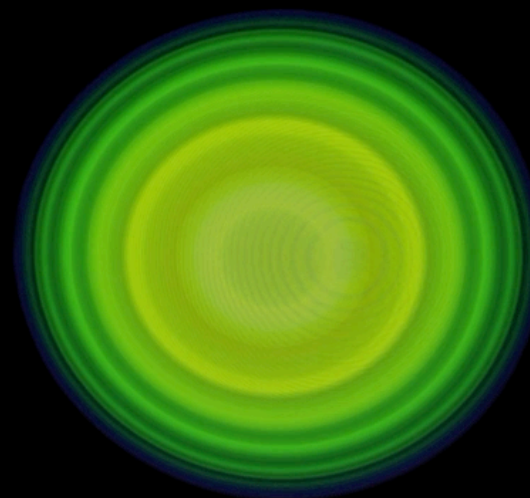
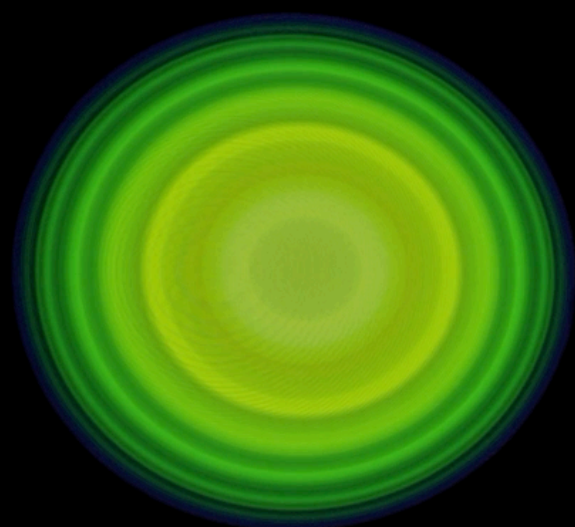


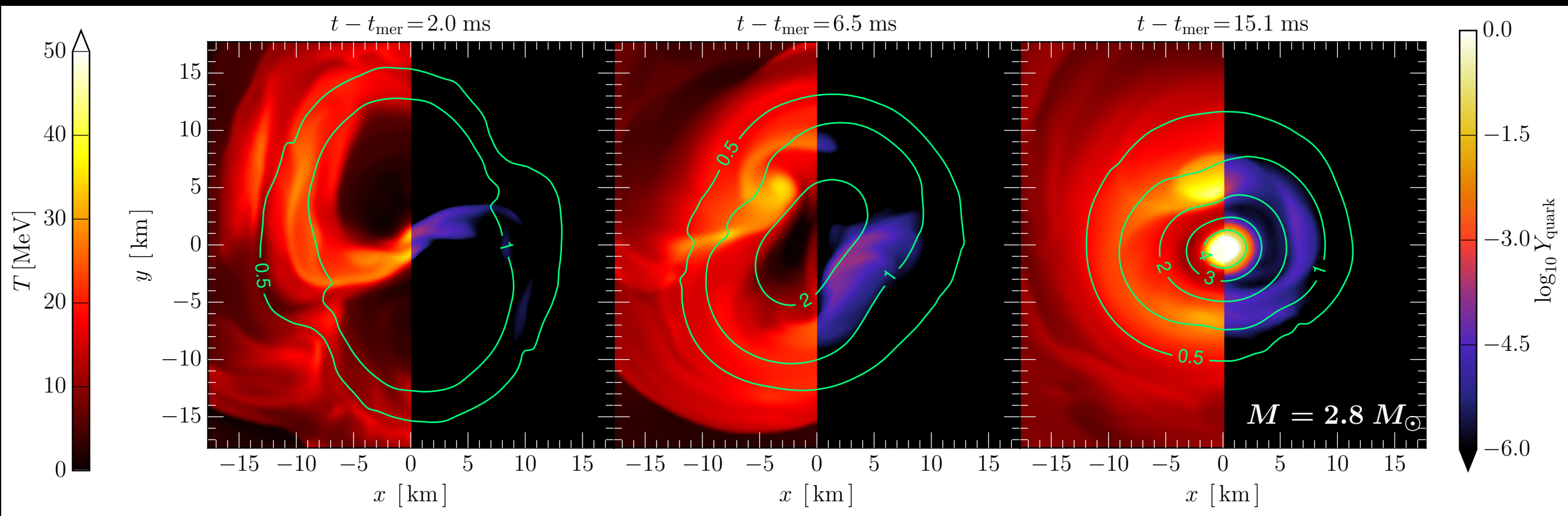
- **Isolated** neutron stars probe a small fraction of phase diagram.
- Neutron-star **binary** mergers reach temperatures up to **80 MeV** and probe regions complementary to experiments.



- Considered EOS based on Chiral Mean Field (CMF) model, based on a nonlinear $SU(3)$ sigma model.
- Appearance of quarks can be introduced naturally.

Animations: Weih, Most, LR

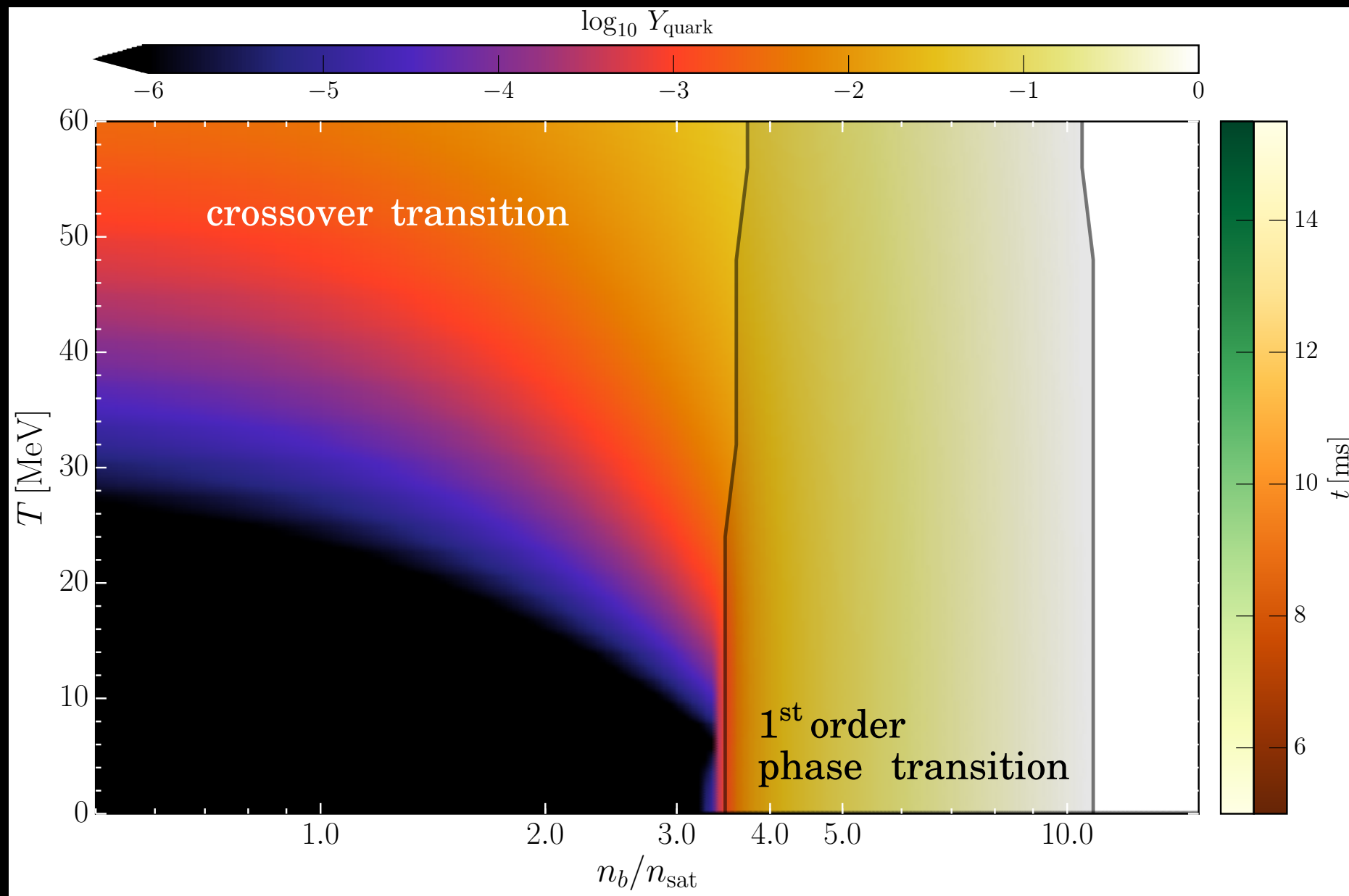




Quarks appear at sufficiently large
temperatures and **densities**.

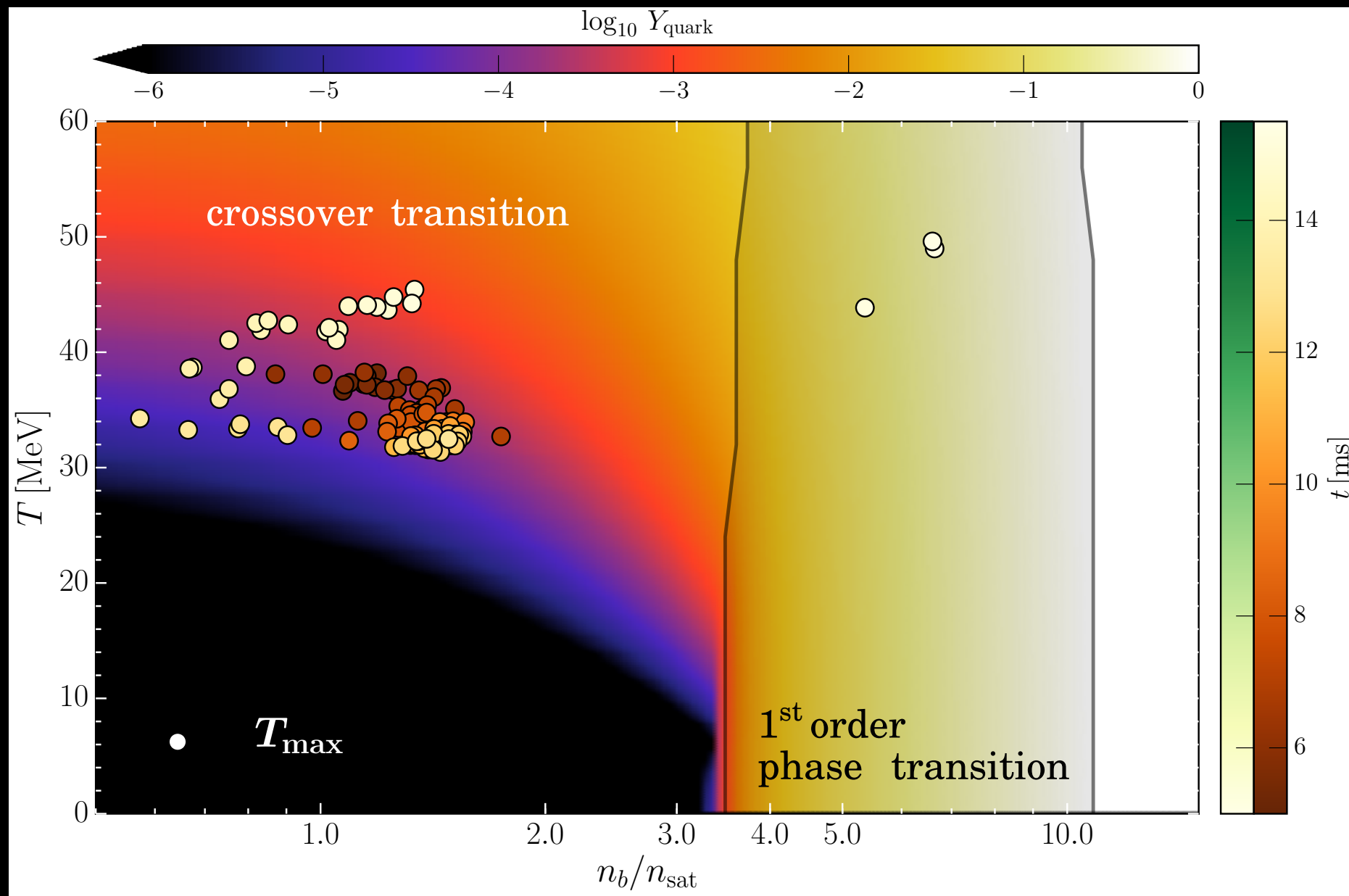
When this happens the **EOS** is
 considerably **softened**.

Comparing with the phase diagram



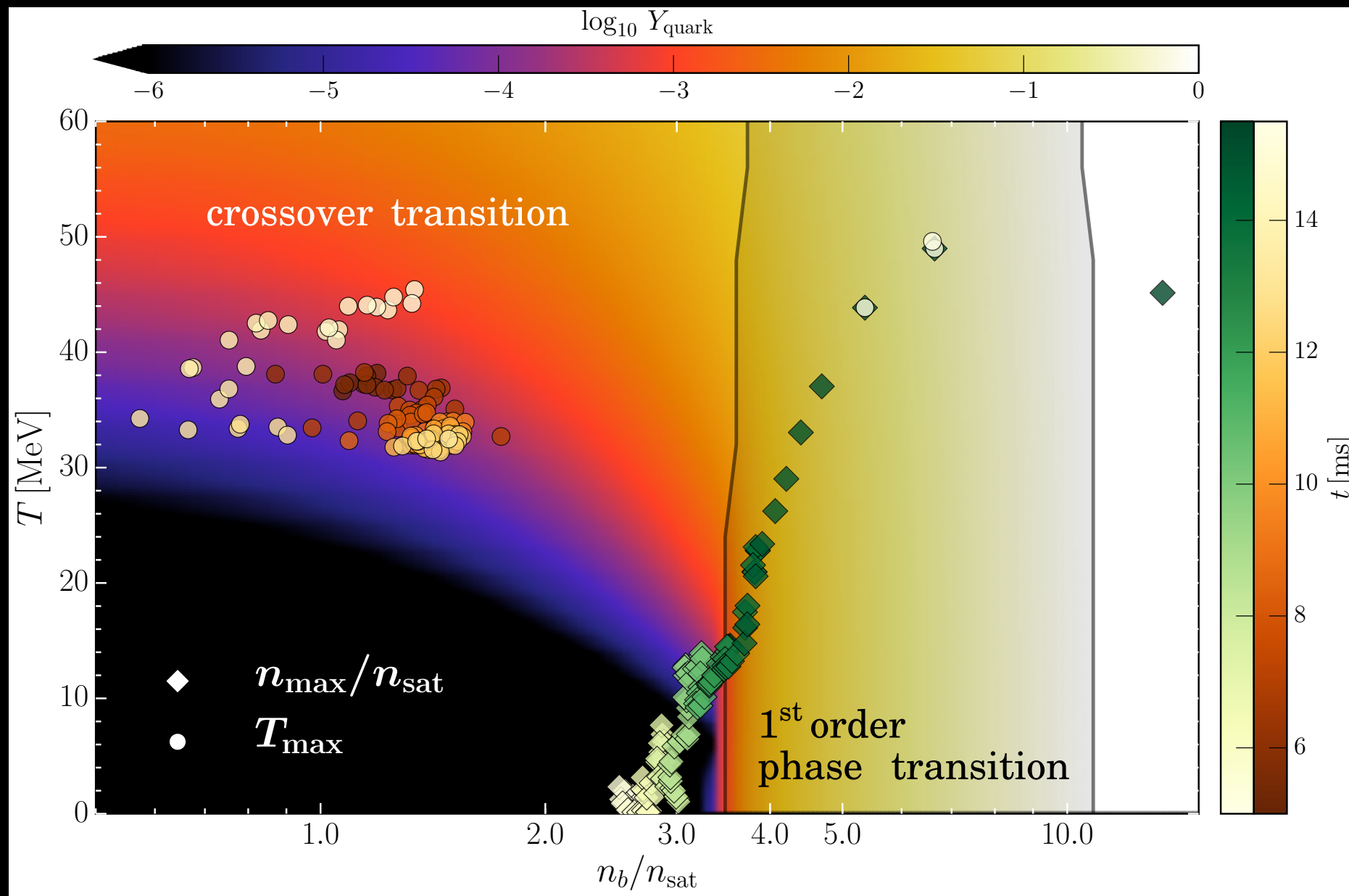
- Phase diagram with quark fraction

Comparing with the phase diagram



- Phase diagram with quark fraction
- Circles show the position in the diagram of the maximum temperature as a function of time

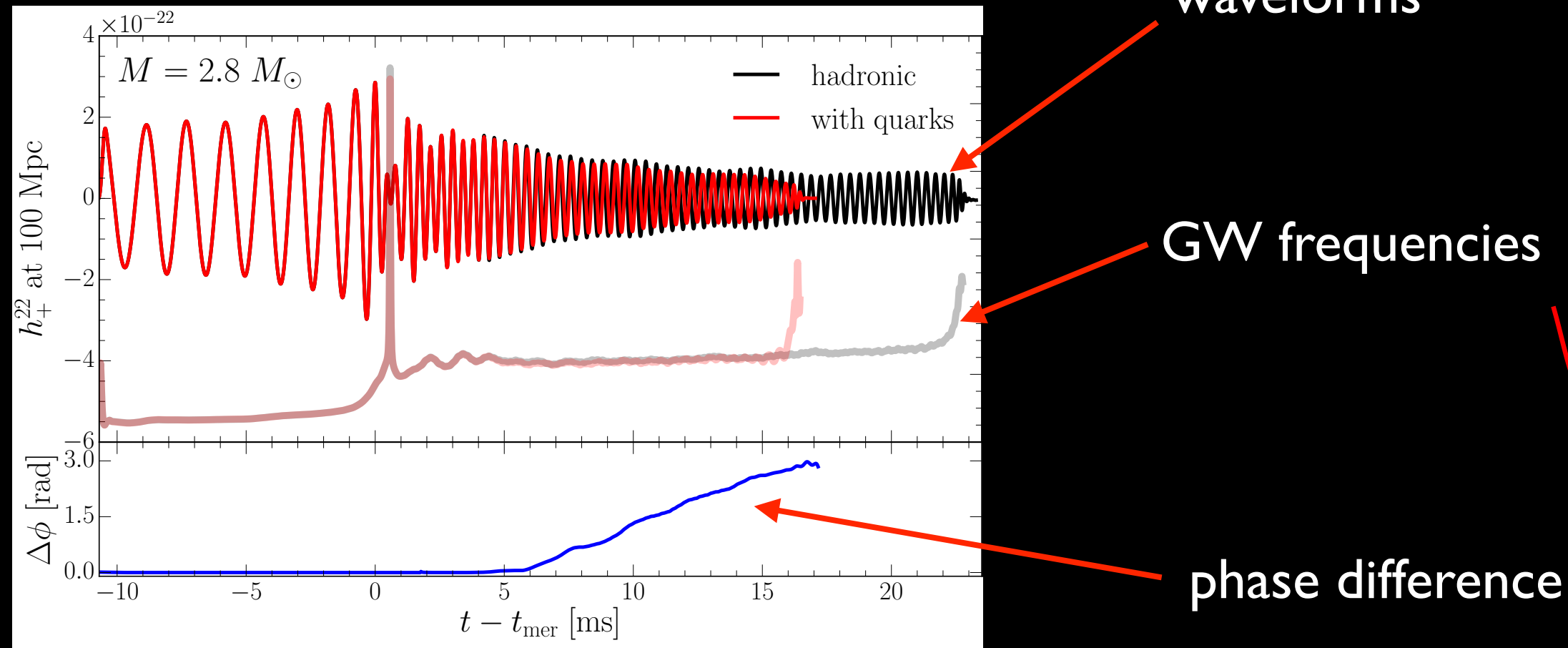
Comparing with the phase diagram



- Reported are the evolution of the max. temperature and density.
- Quarks appear already early on, but only in small fractions.
- Once sufficient density is reached, a full phase transition takes place.

Gravitational-wave emission

“low-mass” binary

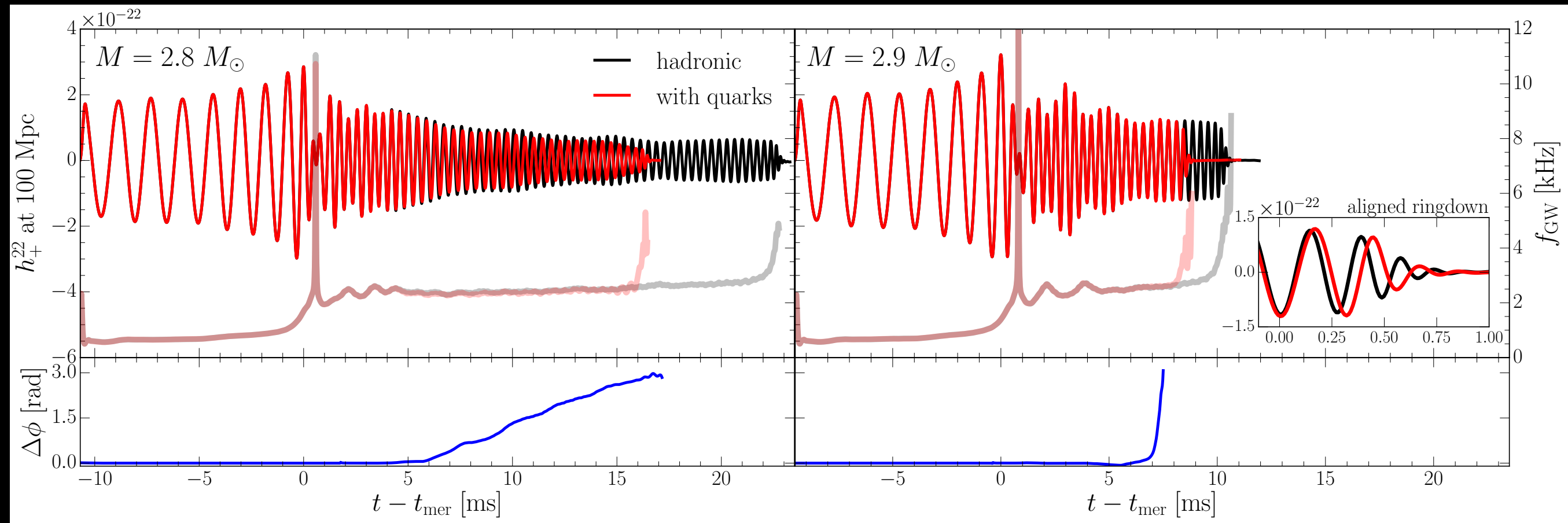


- In **low-mass binary**, after ~ 5 ms, quark fraction is large enough to change quadrupole moment and yield differences in the waveforms.
- Sudden softening of the phase transition leads to collapse and **large difference** in phase evolution.

Gravitational-wave emission

“low-mass” binary

“high-mass” binary



- In **low-mass binary**, after ~ 5 ms, quark fraction is large enough to change quadrupole moment and yield differences in the waveforms.
- In **high-mass binary**, phase transition takes place rapidly after ~ 5 ms. Waveforms are similar but **ringdown** is **different** (free fall for PT). Observing mismatch between **inspiral** (fully hadronic) and **post-merger** (phase transition): clear **signature** of a **PT**

Conclusions

- * Spectra of post-merger shows peaks, some **"quasi-universal"**.
- * When used together with tens of observations, they will set tight constraints on EOS: radius known with **~1 km** precision.
- * Merging binaries with magnetic fields can lead to the formation of **jet structures** and match phenomenology of SGRBs.
- * **GW170817** has already provided new limits on
 - $2.01^{+0.04}_{-0.04} \leq M_{\text{TOV}}/M_{\odot} \leq 2.16^{+0.17}_{-0.15}$ **maximum mass**
 - $12.00 < R_{1.4}/\text{km} < 13.45$ $\tilde{\Lambda}_{1.4} > 375$ **radius, tidal deformability**
 - $M_{\text{th}}/M_{\text{TOV}} \approx 1.41$ $R_{\text{TOV}} \geq 9.74^{+0.14}_{-0.04} \text{ km}$ **threshold mass**
- * A phase transition after a BNS merger leaves GW **signatures** and opens a gate to access quark matter beyond accelerators